WIDEBAND HF NOISE/INTERFERENCE MODELING PART II: HIGHER ORDER STATISTICS

John J. Lemmon and Christopher J. Behm*

This report is the second in a series of reports which describe the development of a wideband HF noise/interference model. The model is based on measured data and is suitable for implementation in a wideband HF channel simulator. The measured data, analyses of the first-order statistics of the data, and a proposed noise/interference model based upon those analyses were discussed in Part I of this series. The present report, Part II of the series, describes analyses of selected higher-order statistics of the data: the autocorrelation function and pulse width and pulse spacing distributions. Examples of these quantities generated from the model are compared with measured data, and refinements of the model based upon analyses of the higher-order statistics are discussed.

Key words: channel simulator; noise/interference; wideband HF

1. INTRODUCTION

1.1 Background

During the past several years interest in HF communication systems over wide bandwidths (on the order of 1 MHz or more) has been revitalized. This resurgence of interest in wideband HF has been motivated by the application of spread spectrum technology to HF systems and the development of digital signal processing techniques which enable the development of HF systems having far better performance than HF systems of only a few years ago.

In view of the numerous uncertainties concerning the performance of new communication systems which have not been fielded and tested extensively, channel simulation is an attractive approach for the evaluation of communication system performance. Channel simulation enables the laboratory performance evaluation of communication systems without the cost and time of building hardware and running extensive field tests. Other advantages of channel simulation, including accuracy, repeatability, stationarity, availability, and parameter variation, have been discussed by Hoffmeyer and Vogler (1987).

---

*The authors are with the Institute for Telecommunication Sciences, National Telecommunications and Information Administration, U.S. Department of Commerce, Boulder, CO 80303-3328.

For a number of years, laboratory performance evaluations of narrowband HF communication systems have been conducted using the channel model and channel simulation techniques developed by Watterson et al. Although this narrowband model and its implementation in channel simulators has been widely reported in the literature (Watterson, 1981 and 1982; Watterson and Coon, 1962; Watterson et al., 1962 and 1970; CCIR, 1974; Ehrman et al., 1982; Mooney, 1985; Girault et al., 1988; McRae and Perkins, 1988; LeRoux et al., 1987), the model has only been validated for narrowband (less than 12 kHz) stable channels.

Motivated by the need for a wideband HF channel simulator, the Institute for Telecommunication Sciences has undertaken the development of a wideband HF channel model. The model is to be accurate over wide bandwidths (on the order of 1 MHz or more), validated with measured data, and suitable for implementation in a wideband HF channel simulator. The model is to include noise and interference, which can be quite severe in the HF band, as well as a model of ionospheric skywave propagation.

The wideband propagation model and the implementation of the propagation and noise/interference models in a real-time channel simulator have been discussed elsewhere (Vogler et al., 1988; Vogler and Hoffmeyer, 1988 and 1990; Hoffmeyer and Vogler, 1990; Hoffmeyer et al., 1991; Mastrangelo et al., 1991). The purpose of the present series of reports is to discuss the development of a wideband HF noise/interference model.

1.2 Noise/Interference Model

In Part I of this series (Lemmon and Behm, 1991) a wideband HF noise/interference model based on measured data was presented. It was pointed out that, in contrast to previously developed models which attempt to describe statistical characteristics of the noise/interference, the present model describes the noise/interference waveform itself, which is essential if the model is to be used to simulate that waveform.

The measured data were obtained by the Mitre Corporation as part of its experimental wideband HF communications program. The equipment used in the experiments was described briefly in Part I and in more detail by Perry and Rifkin (1989). The data consist of 42 one-second records of the digitized (sampled at 1.024 MHz), baseband, in-phase (I) and quadrature (Q) components of the received noise/interference over an equivalent rf bandwidth of 800 kHz.

The data were collected in March, 1989 in Bedford, MA at various times of day and at various frequencies in the HF band (3-30 MHz). The times, dates, center frequencies of the data, and the values of the variable attenuation used in the front-end of the receiver are listed in Table A-1 in the Appendix.

To analyze these data, software was developed to generate the following quantities:

- plots of raw data (I and Q)
- probability density function (pdf) of raw data
- pdf of voltage envelope ($\sqrt{(I^2+Q^2)}$)
- pdf of power envelope (I^2+Q^2)
- pdf of phase ($\tan^{-1}Q/I$)
- cumulative distribution function (cdf) of power envelope
- distribution of average level crossing rate of the voltage envelope
- power spectrum
- cdf of power in the frequency domain (sum of the squares of the real and imaginary parts of the complex Fourier transform of the raw data)
- pdf of phase in the frequency domain (phase of the complex Fourier transform of the raw data)

In addition, software was developed to perform the following functions:

- frequency domain excision of narrowband interference
- simulations of noise/interference

Using these analysis tools, a variety of case studies were conducted. Based on the results of the case studies, it was proposed that the noise/interference can be represented as a sum of three components:

- Gaussian noise
- Narrowband interferers (sine waves)

Impulsive noise (filtered delta functions)

The narrowband interference is presumably manmade, arising from numerous users of the HF band. Broadband impulsive noise can be natural (atmospheric noise) or manmade. However, as discussed in Section 3, the impulsive noise analyzed herein is assumed to be of manmade origin, because the time durations of the noise bursts and the times between bursts are not consistent with those of atmospheric noise.

If x(t) denotes the noise/interference signal at rf, and the in-phase and quadrature components of the baseband signal are denoted by I(t) and Q(t), respectively, then x(t) can be written as

$$x(t) = I(t)\cos \omega_0 t + Q(t) \sin \omega_0 t, \qquad (1)$$

where ω_0 is the carrier frequency. The proposed noise/interference model describes the complex baseband voltage,

$$z(t) = I(t) + iQ(t), \qquad (2)$$

by the expression

$$z(t) = g(t) + \sum_{i=1}^{N_i} A_i e^{-i(\Delta\omega_i t + \phi_i)} + \sum_{j=1}^{N_j} B_j \frac{\sin 2\pi B(t-t_j)}{t-t_j} e^{i\omega_0 t_j}, \qquad (3)$$

where g(t) is a complex, zero-mean, white Gaussian process, $\Delta\omega_i$ are the baseband frequencies of the sine waves ($\Delta\omega_i=\omega_i-\omega_0$), ,$\phi_i$ are random phases, B is the bandpass (in Hz) of the low-pass filter in the HF receiver, t_j are the arrival times of the (filtered) impulses, N_i is the number of narrowband interferers in the frequency band of interest, and N_j is the number of impulses in the time interval over which the noise/interference is being modeled. The frequency and phase distributions of the narrowband interferers are uniform, and in Part I the arrival times t_j were also uniformly distributed, although it will be shown in the present report that this is inadequate to

correctly model the higher-order statistics.

It remains to specify how the amplitudes A_i and B_j are distributed. In Part I it was proposed that the pdf for the amplitudes A_i be modeled by the amplitude pdf of a model developed by Hall (1966):

$$p(A) = \frac{(\theta_A - 1)\,\gamma_A^{\theta_A - 1}\,A}{(A^2 + \gamma_A^2)^{(\theta_A + 1)/2}}, \qquad (4)$$

where θ_A and γ_A are free parameters (with the constraint that $\theta_A > 1$, so that p(A) is normalizable). It was also proposed in Part I that the amplitude distribution of the B_j be described by that of the Hall model for amplitudes which are less than some maximum value B_{max}, and that the distribution be cut off for amplitudes greater than B_{max}:

$$p(B) = \begin{cases} \dfrac{1-\theta_B}{(B_{max}^2+\gamma_B^2)^{(1-\theta_B)/2} - \gamma_B^{2(1-\theta_B)/2}} \cdot \dfrac{B}{(B^2+\gamma_B^2)^{(\theta_B+1)/2}}, & 0 \le B \le B_{max} \\ 0, & B > B_{max} \end{cases}, \qquad (5)$$

where θ_B and γ_B are free parameters (with $\theta_B > 1$). The expression in the first line of (5) differs from that in (4) because cutting off the distribution results in a different normalization constant. The techniques used to generate amplitudes distributed according to (4) and (5), and to generate the Gaussian noise, were discussed in Part I.

1.3 Scope

The model described above enables one to simulate noise/interference signals whose statistical characteristics can be compared to those of measured data. Clearly, many such characteristics could be examined. In Part I of this series, the first-order statistics were investigated. These quantities characterize the time-averaged behavior of the noise/interference. It was shown that, for appropriate values of the model parameters, the simulated noise/interference has first-order statistics that closely resemble those of the measured data.

However, a complete characterization of the noise/interference requires investigation of the higher-order statistics as well. These statistics are necessary to specify the relationships between the noise/interference process at different instants in time. For example, it was shown that the average numbers of level crossings of the voltage envelope per unit time of the simulated noise/interference are in agreement with measured data, but it remains to investigate how these envelope crossings are distributed in time.

In this report, selected higher-order statistics of the noise/interference are discussed. To keep the analysis tractable, attention has been restricted to the following three quantities:

- Autocorrelation functions
- Pulse width distributions
- Pulse spacing distributions

Autocorrelation functions are important because they define the time scales over which the noise/interference becomes decorrelated and provide information about the time scales over which the noise/interference processes vary. Pulse width and spacing distributions are useful for detailed modeling of the noise/interference waveforms, especially impulsive noise. These distributions provide information about the fine structure of the noise bursts, as well as information about the nature of the correlations of the noise bursts in time.

2. AUTOCORRELATION FUNCTIONS

2.1 Calculation of the Autocorrelation Function

The autocorrelation function is of fundamental significance in characterizing a random process because it specifies the degree to which the process is correlated at different instants in time. For a general (nonstationary) complex-valued random process z(t), the autocorrelation function $\gamma_{xx}(t_1,t_2)$ at times t_1 and t_2 is defined as (for example,see Cox and Miller, 1965):

$$\gamma_{xx}(t_1,t_2) = E\{x(t_1)x(t_2)\}, \qquad (6)$$

where E{ }, the expected value, is defined as an ensemble average, and where * denotes the complex conjugate.

For the case of a stationary process, $\gamma(t_1,t_2)$ is not a function of t_1 and t_2 separately, but is a function of the time difference $\tau=t_2-t_1$. For the case of a stationary, ergodic process, the ensemble average is equivalent to a time average so that the autocorrelation function, denoted by $R(\tau)$, can be defined as:

$$R(\tau) = \lim_{T\to\infty}\frac{1}{T}\int_0^T z^*(t)z(t+\tau)dt, \qquad (7)$$

The noise/interference data to be analyzed consist of 42 one-second records that were collected at various times of day and at various frequencies in the HF band. Thus, for a given time and frequency, only one data record is available (not an ensemble of records), so that the ensemble average in (6) cannot be computed. On the other hand, the expression in (7) cannot be evaluated, because a record of infinite length is not available, and because the computational effort would be prohibitive for arbitrarily large, but finite T. Moreover, the noise/interference is generally nonstationary, so that the definition in (7) is not applicable. For example, Abraham et al. (1989) investigated the nonstationarity of wideband (1 MHz) HF noise after interference

excision and found, using a standard statistical F-test, that average stationary time durations were only on the order of 10 ms.

These difficulties are often encountered in the calculation of autocorrelation functions. An alternative approach that is commonly used is to calculate the quantity $R(\tau,T)$, defined as

$$R(\tau,T) = \frac{1}{T}\int_0^T z^*(t)z(t+\tau)dt. \qquad (8)$$

For a stationary, ergodic process $R(\tau,T)$ approaches $\gamma(\tau)$ as T approaches infinity. However, this is not the case for a nonstationary process, and therefore $R(\tau,T)$ is not a true autocorrelation function in the strict sense, even as T approaches infinity. Nevertheless, $R(\tau,T)$ is a useful measure of the degree to which a random process is correlated with itself at different instants of time, and this is the definition of the autocorrelation function used in this work.

An analytic expression for $R(\tau,T)$ in the proposed noise/interference model can be obtained by substituting (3) into (8). First consider R(0,T). The Gaussian noise, the narrowband interferers, and the impulsive noise are uncorrelated with one another, and the Gaussian noise and the narrowband interferers are zero-mean processes. Therefore, upon substituting (3) into (8), the integrals of the cross-terms between the Gaussian noise and the narrowband interferers, between the narrowband interferers and the impulsive noise, and between the Gaussian noise and the impulsive noise vanish. Thus, R(0,T) is simply the sum of the average power of the Gaussian noise, the narrowband interferers, and the impulsive noise. These integrals are easily performed, and were discussed in Part I. The results are:

$$P_G = 2\sigma^2 \qquad (9)$$

where σ^2 is the variance of the real and imaginary parts of g(t),

$$P_{NB} = \sum_{i=1}^{N_I} A_i^2 \qquad (10)$$

and

$$P_{IMP} = \frac{2\pi^2 B}{T} \sum_{j=1}^{N_J} B_j^2 . \qquad (11)$$

Now consider $R(\tau,T)$ for non-zero values of τ. Again, the integrals of the cross-terms between different components of the noise/interference vanish, leaving the sum of the autocorrelation functions of the individual components.

The Gaussian noise is white; hence, its power spectrum is independent of frequency, and its autocorrelation function (the inverse Fourier transform of the power spectrum) is a delta function. Therefore, the autocorrelation function of the Gaussian noise vanishes for non-zero values of τ.

The impulsive noise consists of filtered impulses which are localized, oscillatory functions of time. Therefore, the only contributions to the autocorrelation function of the impulsive noise arise at those values of τ that equal the difference of the times of arrival of two distinct impulses. Let two such impulses be labeled by a and b. Then the corresponding contribution to the autocorrelation function is:

$$\frac{2\pi^2 B}{T} B_a B_b e^{i\omega_0 (t_b - t_a)} \qquad (12)$$

where the integral from 0 to T has been approximated by the integral from $-\infty$ to $+\infty$. If the impulses arrive periodically in time, contributions of the form of (12) combine at values of τ which are integral multiples of the period. However, the arrival times of the impulses in the data analyzed herein are not precisely periodic, and therefore contributions of the form of (12) do not combine for non-zero τ. Moreover, it was shown in Part I that accurate simulation of the data containing impulsive noise required approximately 50 impulses over a duration of 4 ms. Thus, if T is on the order of or greater than 4 ms (which it is in the examples below), contributions of the form of (12) are expected to be small compared to the sum in (11). It was also shown in the aforementioned simulation in Part I that the sum in (11) is itself approximately 11 dB less than

the contribution in (10) due to the narrowband interferers. Therefore the autocorrelation function of the impulsive noise is expected to approximately vanish for non-zero τ.

Finally, the autocorrelation function of the narrowband interferers is readily evaluated. One has:

$$\sum_{i=1}^{N_I} A_i^2 e^{-i\Delta\omega_i\tau}, \tag{13}$$

where the integral over the cross-terms vanishes due to the orthogonality of sines and cosines of different frequencies.

Combining results, the complete autocorrelation function of the noise/interference model can be approximated as:

$$R(\tau,T) = (2\sigma^2+\frac{2\pi^2 B}{T}\sum_{j=1}^{N_J} B_j^2)\,\delta_{\tau,0} + \sum_{i=1}^{N_I} A_i^2 e^{-i\Delta\omega_i\tau}, \tag{14}$$

where $\delta_{\tau,0}$ is an impulse function, defined as:

$$\delta_{\tau,0} = \begin{cases} 1, & \tau=0 \\ 0, & \tau\neq 0 \end{cases}. \tag{15}$$

Thus, $R(\tau,T)$ consists of an impulse at $\tau=0$, and the periodic function in (13) at non-zero values of τ.

2.2 Comparisons of Model with Measurements

In Part I of this series, the 42 noise/interference records were examined, and five records were selected that were considered to be representative of the entire data base. Detailed case studies (consisting of analyses of the first-order statistics) were performed on these five records. The results of two of the case studies were compared with analyses of the first-order statistics of simulated noise/interference for two particular sets of model parameters. A similar program was carried out in the present work for the higher-order statistics. The times, dates, and center

frequencies for the five case studies are listed in Table 1. The autocorrelation function for each of the five case studies was computed using (8). The integration time T was chosen to be 4 ms (i.e., 4096 samples). For each case the autocorrelation function was computed for $0 \leq \tau \leq 8$ ms and 0.996 s $\leq \tau \leq$ 1.004 s, corresponding to two 8 ms windows of delay at the beginning and end of each one-second record. Because one expects an impulse in $R(\tau,T)$ at $\tau=0$, which is difficult to see on the plots, the autocorrelation functions were normalized so that $R(0,T)=1$. Finally, because $R(\tau,T)$ is complex, the absolute magnitudes of the normalized autocorrelation functions have been plotted. Thus, the quantity which has been plotted in each case is $|R(\tau,T=4 \text{ ms})/R(0,T=4 \text{ ms})|$.

To gain some insight into the nonstationarity of the noise/interference, the power (I^2+Q^2) has been plotted versus time for each of the 42 one-second records. The results are shown in the Appendix. Each plot shows the power averaged over 1,024 consecutive samples (i.e., over 1 ms) and plotted (in dB) versus time for the entire one-second record. The time scales on the horizontal axes in these plots are therefore in units of ms. Thus, the "number of 1024 samples" spans an interval of 1024, which corresponds to a time duration of 1.024 s. These plots reveal that, over time intervals of 1 second, the received power is reasonably stationary in some cases, but can be highly nonstationary in others.

Table 1. Measurement Characteristics of Wideband HF Noise/Interference Records Used in Case Studies

Case Study	Date (1989)	Time (UT)	Center Frequency (MHz)
1	10 March	09:58:11	5.936
2	28 March	22:10:40	19.29
3	28 March	10:26:48	13.666
4	29 March	02:31:34	13.666
5	15 March	19:22:32	23.862

The I-channel data, the normalized autocorrelation function, and the average power for the first case study are shown in Figures 1, 2, and 3, respectively. The time scales on the horizontal axes in Figures 1 and 2 are in units of the sample time of the data, that is, 1/1.024 MHz. Thus, the "count" in Figure 1 spans an interval of 4096 samples, which corresponds to a time duration of precisely 4 ms. Similarly, the "delay" in each of the plots in Figure 2 spans an interval of 4096 samples, which corresponds to a range of τ of precisely 4 ms.

The I-channel data in Figure 1, plotted over the first 4 ms of the record, is typical of the 42 noise/interference records. The normalized autocorrelation function in Figure 2 is as expected: a unit impulse at τ=0 followed by a periodic function of τ. By the end of the one-second record the autocorrelation function has changed slightly; this is an indication that the channel was not precisely stationary over the duration of the record, as reflected in the average power plotted in Figure 3.

Figures 4, 5, and 6 show the I-channel data, the normalized autocorrelation function, and the average power, respectively, for the second case study. As in the first case study, the autocorrelation function shows the expected behavior, but varies slightly by the end of the record, due to a small degree of nonstationarity in the channel.

The I-channel data, the normalized autocorrelation function, and the average power for the third case study are plotted in Figures 7, 8, and 9, respectively. Whereas the autocorrelation functions in the other four case studies consist of a rapidly oscillating, periodic function with a well-defined envelope, the function in Figure 8 is neither rapidly oscillating nor periodic, at least over time intervals of 8 ms or less. However, this behavior can easily be accounted for within the proposed noise/interference model.

If the sum over narrowband interferers in (13) and (14) is dominated by a single term, the magnitude of the autocorrelation function is a constant. If the channel is dominated by two narrowband interferers with equal amplitudes and closely spaced in frequency, the resulting signal (beating pattern) consists of a single carrier at the average frequency, amplitude modulated by a sine wave of half the difference frequency. It is easy to show that the magnitude of the resulting autocorrelation function is proportional to the magnitude of the autocorrelation function of the slowly varying modulating function (a sine wave). More complicated modulating functions can arise if additional pairs of narrowband interferers (with equal amplitudes) beat against one

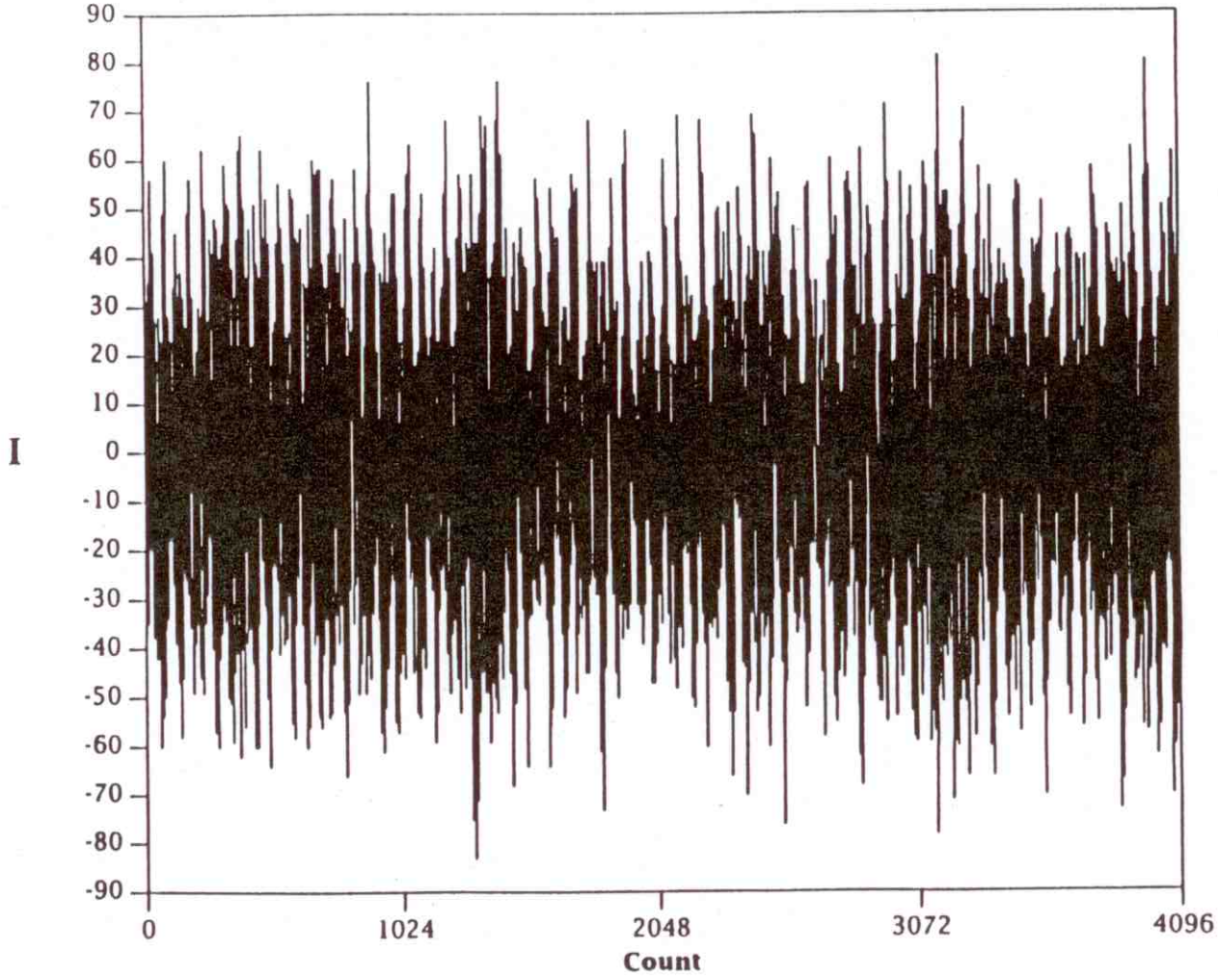

Figure 1. I-channel data at 5.936 MHz (case study 1).

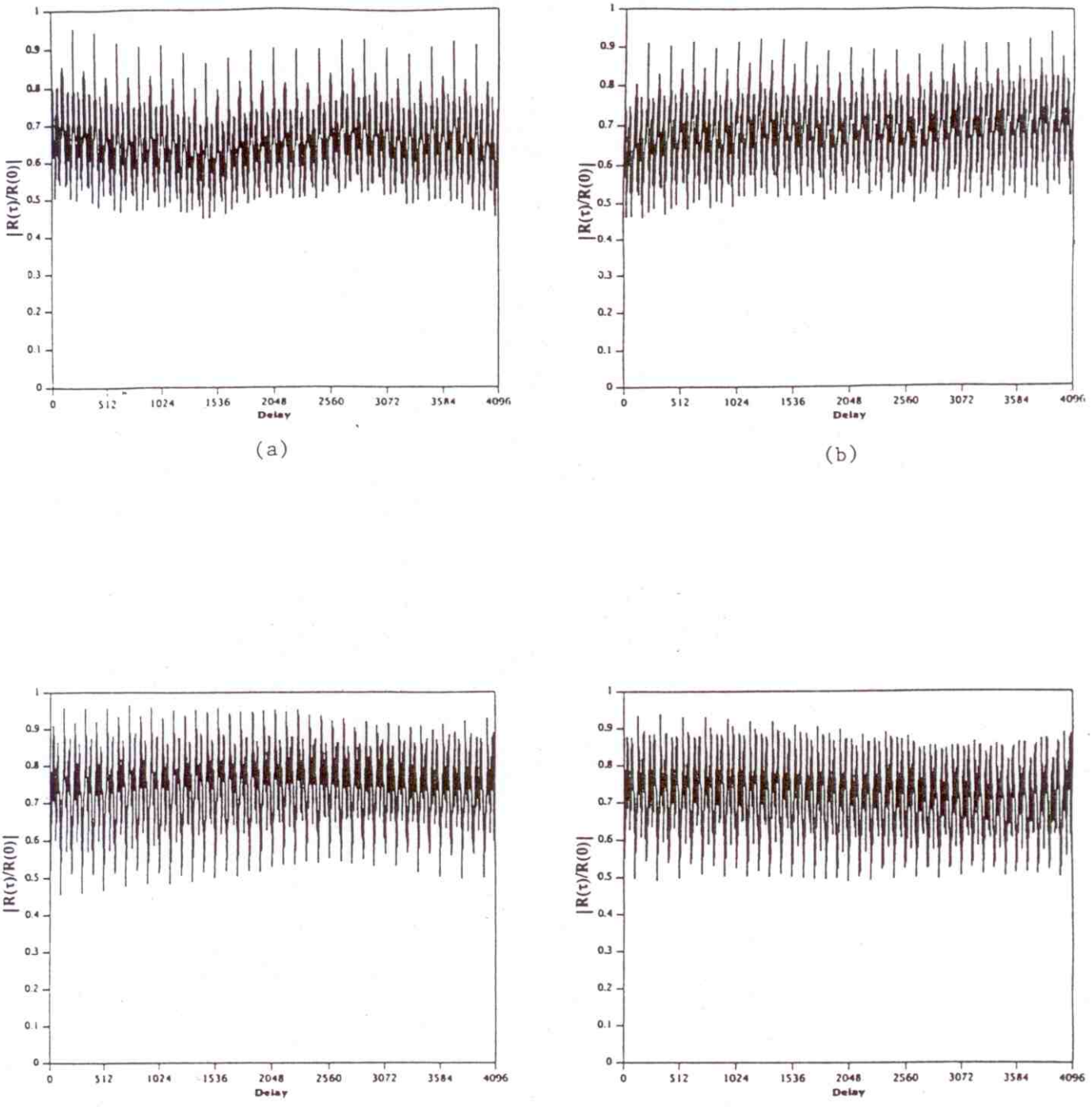

Figure 2. Normalized autocorrelation function for (a) $0 \leq \tau \leq 4$ms, (b) 4ms $\leq \tau \leq 8$ms, (c) 0.996s $\leq \tau \leq$ 1.0s, and (d) 1.0s $\leq \tau \leq$ 1.004s (case study 1).

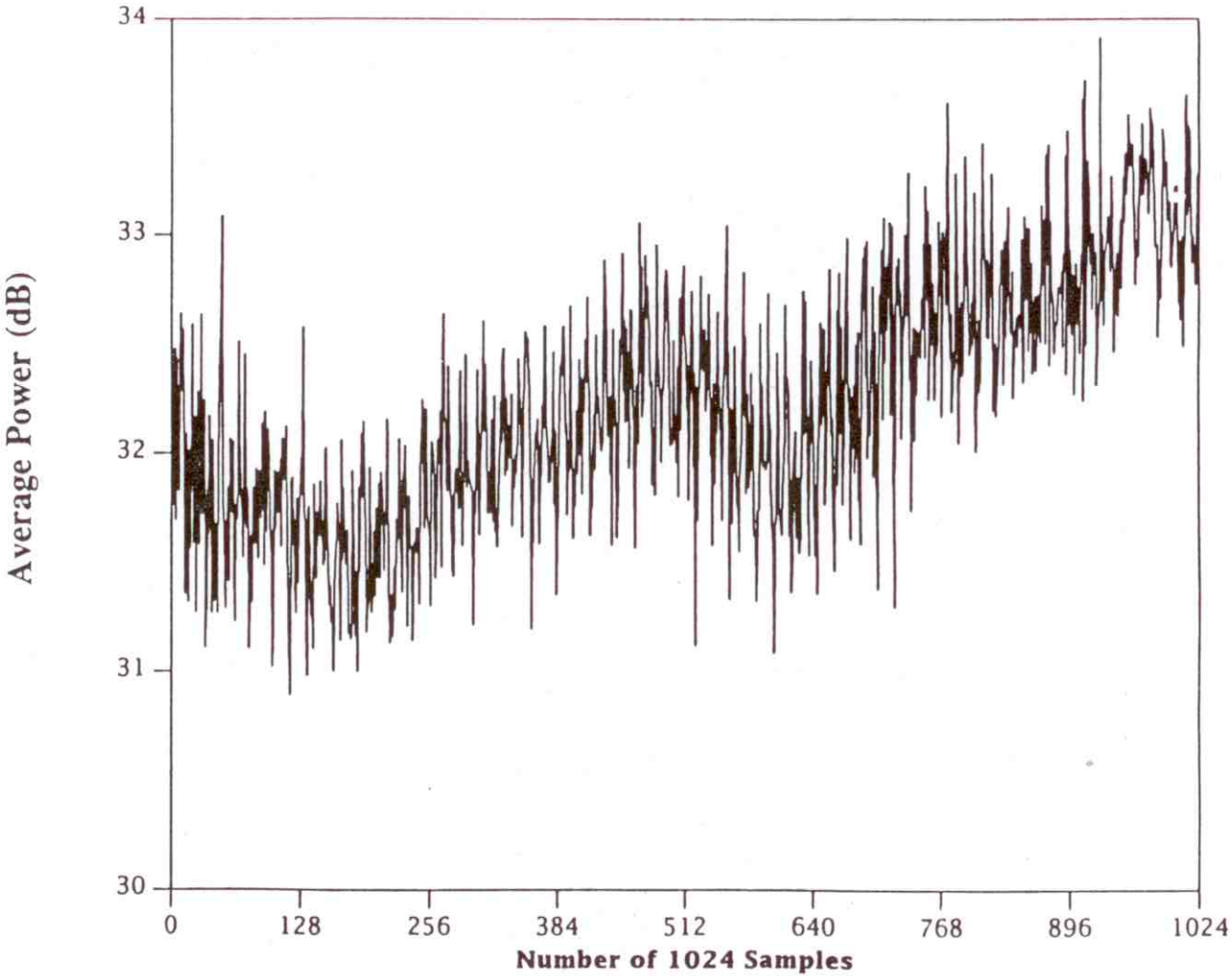

Figure 3. Average power of measured noise/interference (case study 1).

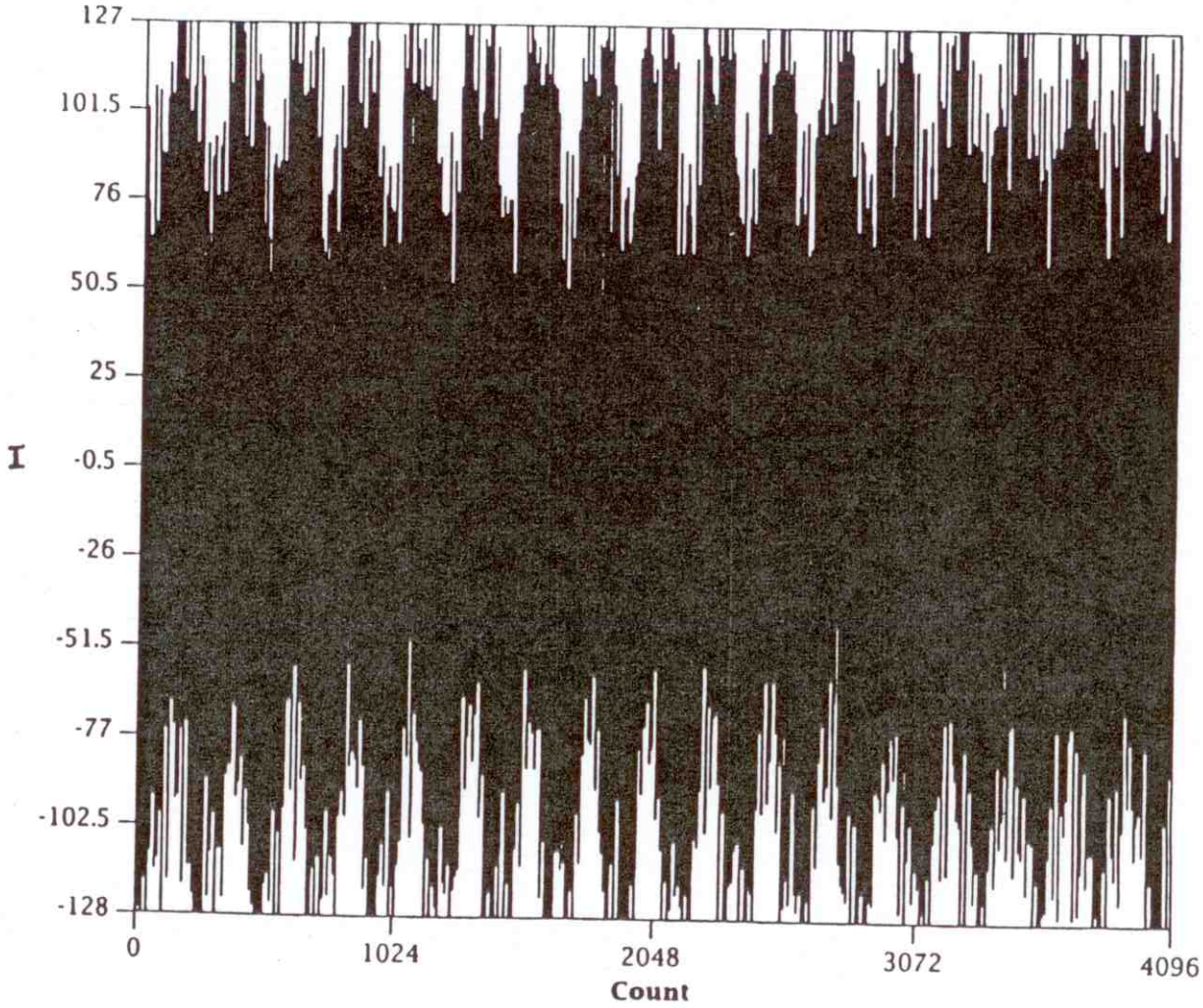

Figure 4. I-channel data at 19.29 MHz (case study 2).

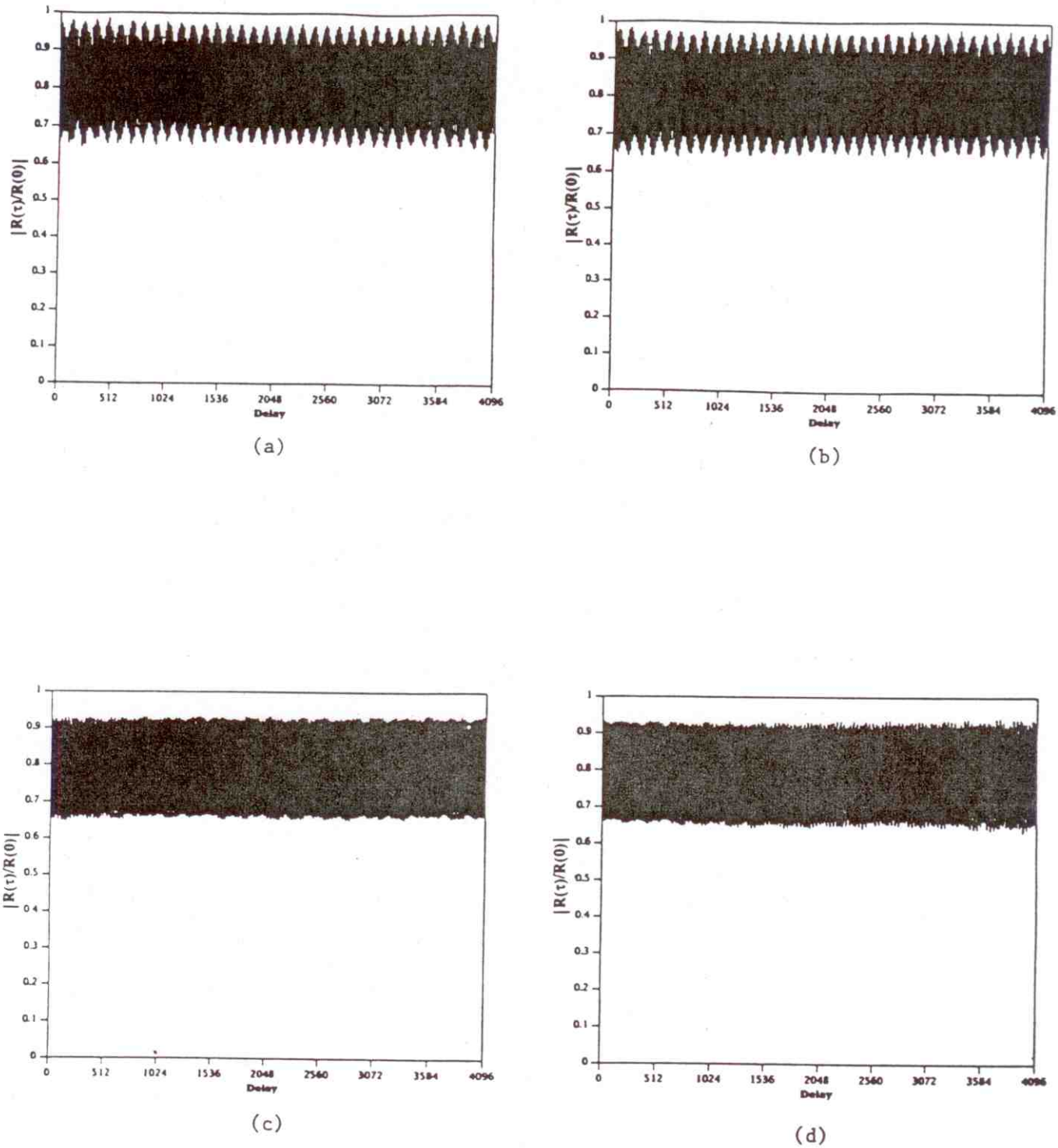

Figure 5. Normalized autocorrelation function for (a) $0 \leq \tau \leq 4$ms, (b) $4\text{ms} \leq \tau \leq 8$ms, (c) $0.996\text{s} \leq \tau \leq 1.0$s, and (d) $1.0\text{s} \leq \tau \leq 1.004$s (case study 2).

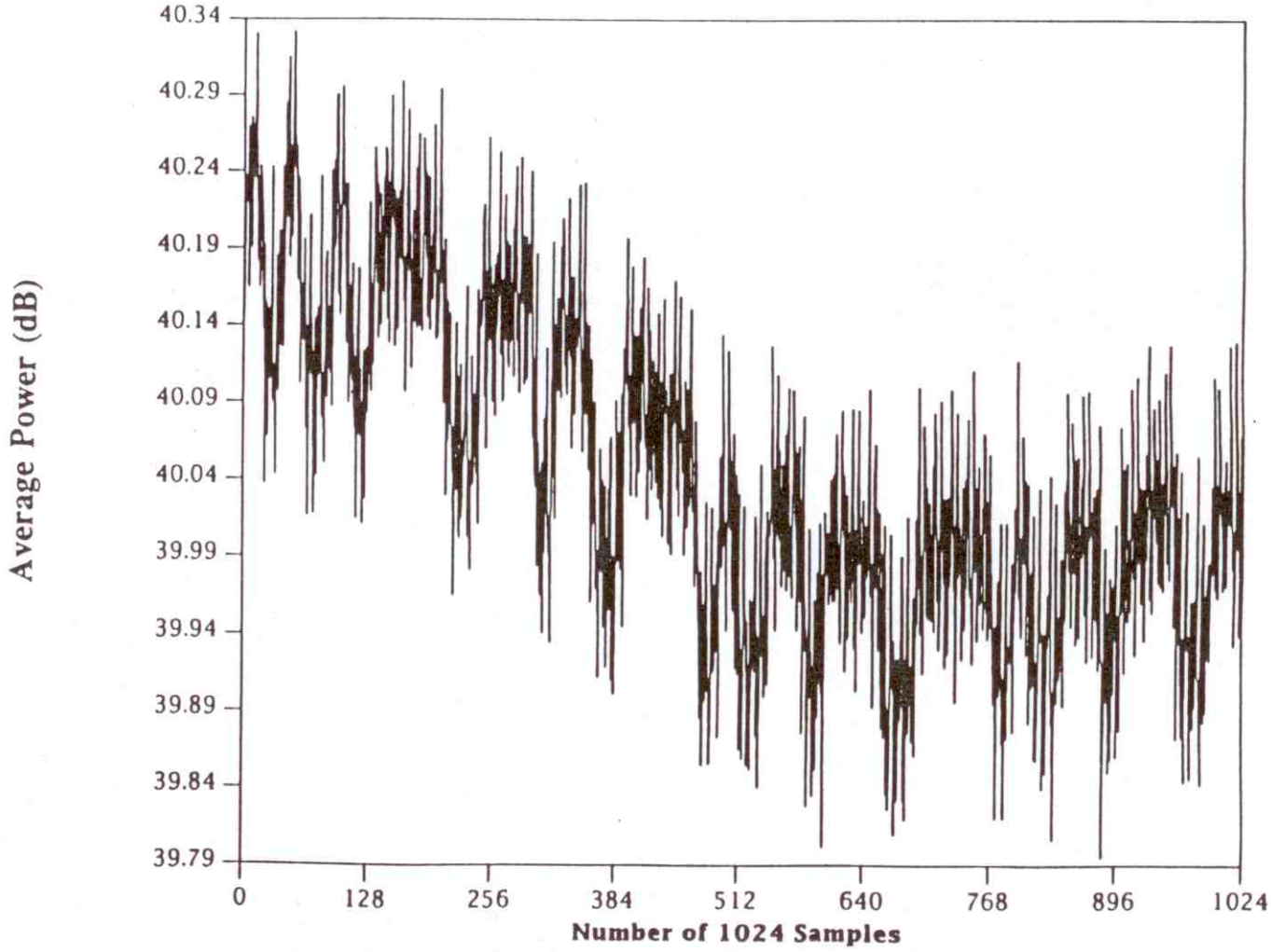

Figure 6. Average power of measured noise/interference (case study 2).

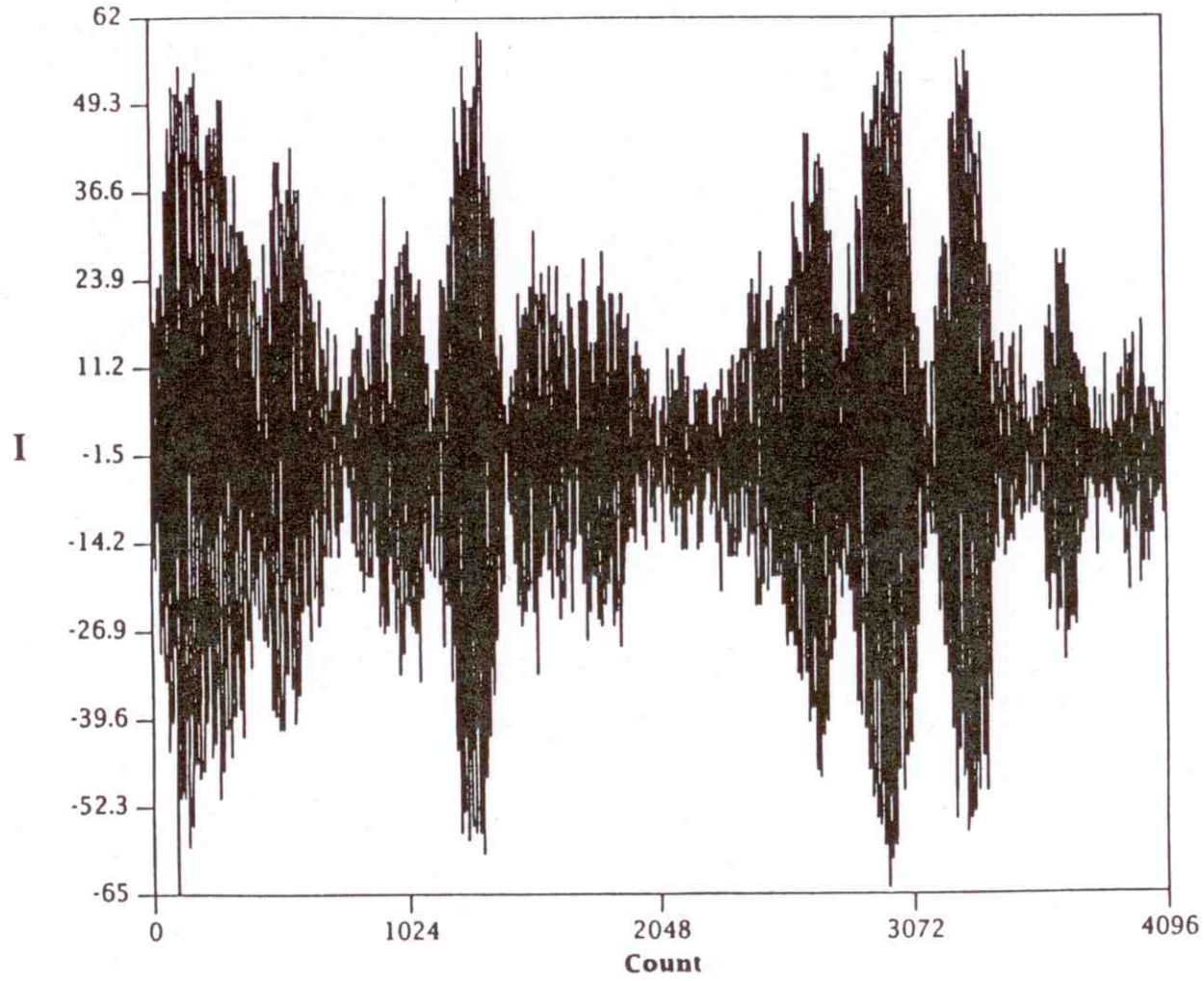

Figure 7. I-channel data at 13.666 MHz (case study 3).

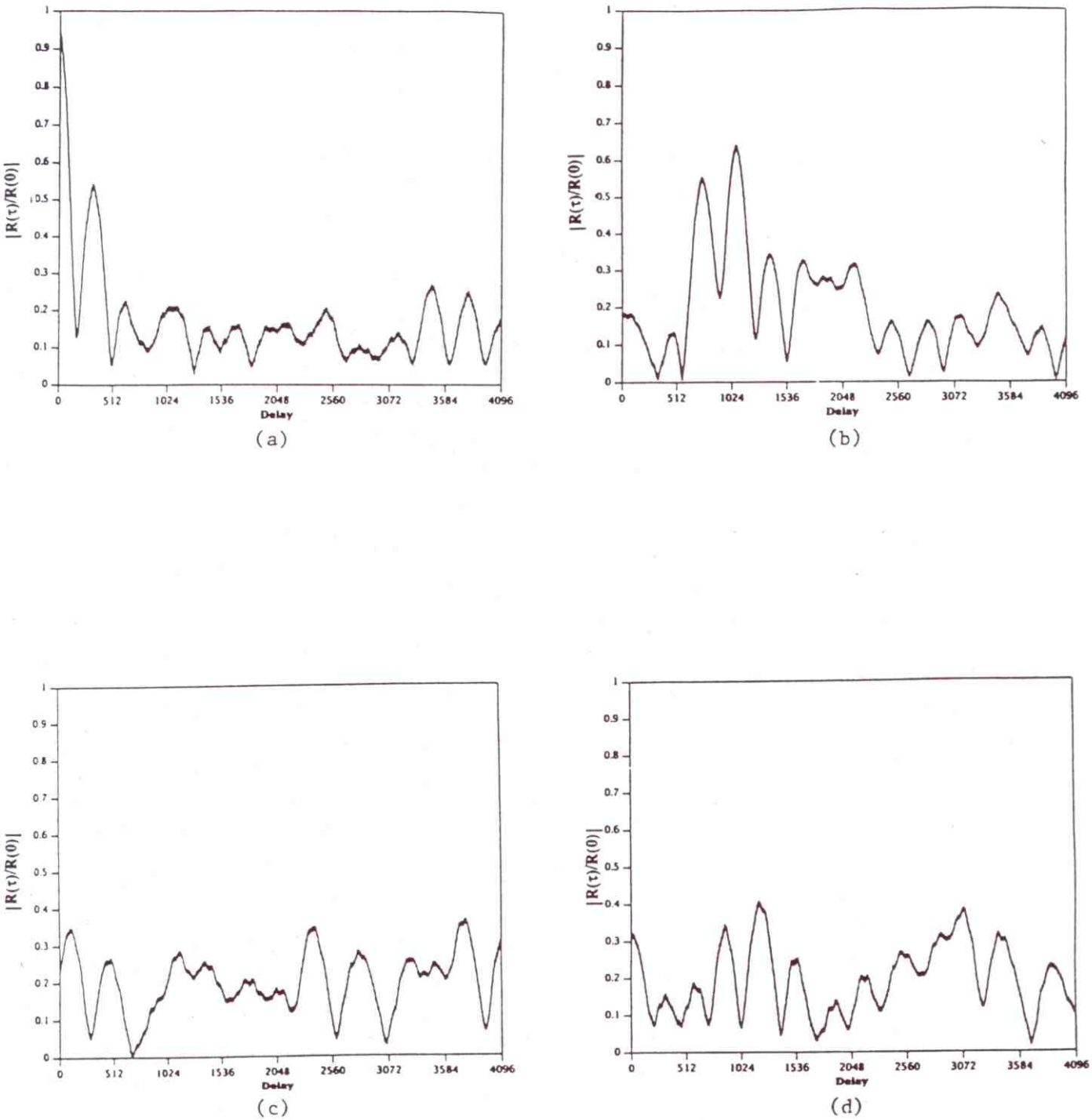

Figure 8. Normalized autocorrelation function for (a) $0 \leq \tau \leq 4$ms, (b) 4ms $\leq \tau \leq$ 8ms, (c) 0.996s $\leq \tau \leq$ 1.0s, and (d) 1.0s $\leq \tau \leq$ 1.004s (case study 3).

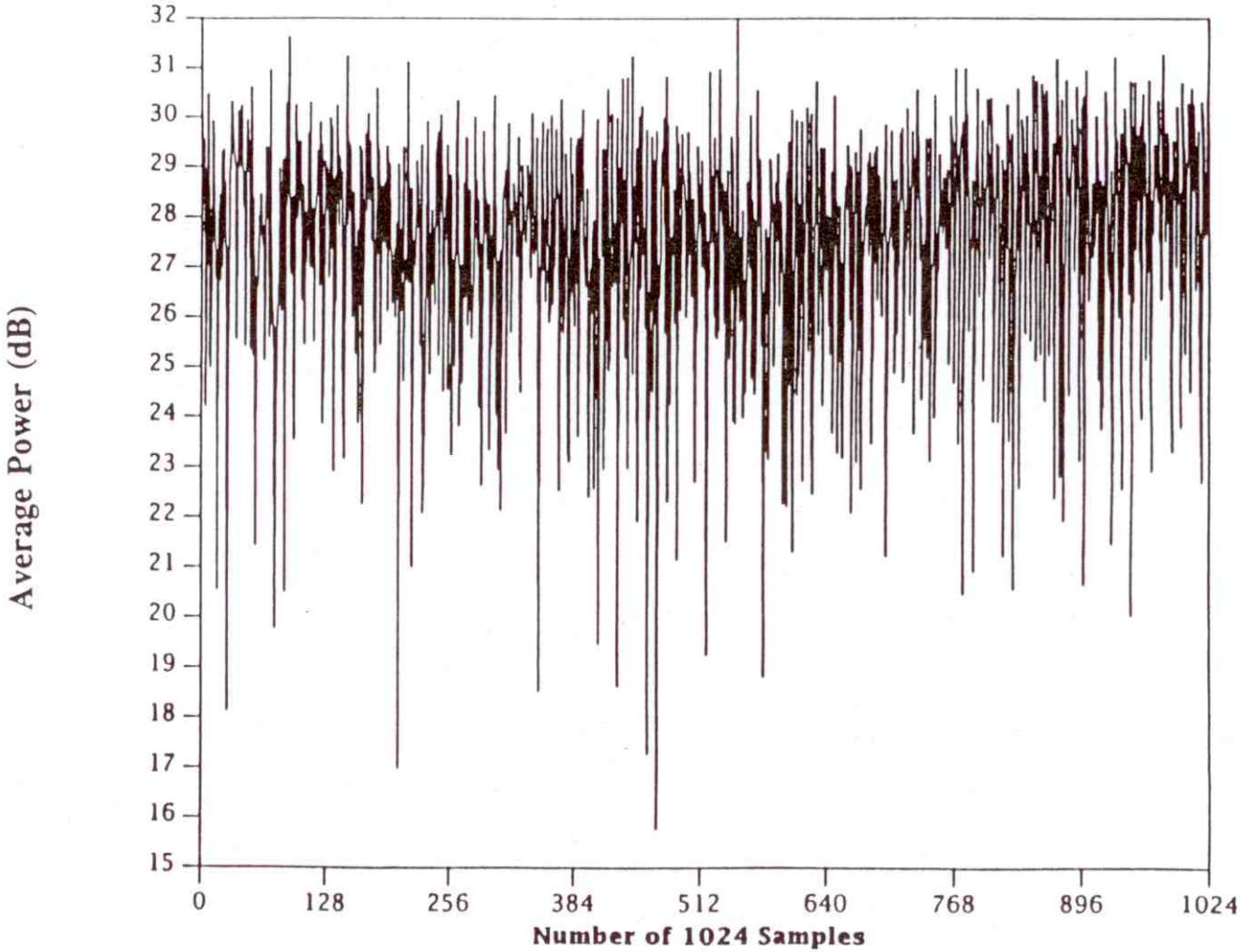

Figure 9. Average power of measured noise/interference (case study 3).

another, such that the average frequency of each pair is the same (so that the resulting signal consists of a single amplitude-modulated carrier).

To take a specific example, consider pairs of narrowband interferers with no random additive phases, distributed symmetrically in amplitude and frequency about some center frequency. The complex baseband signal can be written as:

$$z(t) = \sum_i A_i \left(e^{-i(\Delta\omega_o - \delta_i)t} + e^{-i(\Delta\omega_o + \delta_i)t}\right), \qquad (16)$$

where $\Delta\omega_0$ is the center frequency. Substituting (16) into (8) and carrying out the necessary integrations, one finds:

$$R(\tau, T) = 2e^{-i\Delta\omega_o\tau} \sum_i A_i^2 \cos\delta_i\tau. \qquad (17)$$

Although the expression in (17) is periodic, the period is large if the lowest common multiple of the periods of the cosine waves is large.

To verify that this type of scenario is applicable to the present case study, the power spectrum calculated from the first 4 ms of the data was examined. The power in the channel is indeed dominated by a cluster of narrowband interferers closely spaced in frequency and centered at approximately 65 kHz (baseband). The power spectrum is plotted on an expanded scale from 0 to 128 kHz in Figure 10. The horizontal scale is in units of 250 Hz, because the spectrum was calculated from 4 ms of data. The frequencies of the four strongest interferers appear to be distributed approximately symmetrically about the center of the cluster. It is difficult to determine whether the amplitudes of the dominant interferers are distributed symmetricaly about the center of the cluster, due to the presence of the background noise; however, the structure of the I-channel data (which resembles a single carrier with amplitude modulation) and the autocorrelation function (which is essentially devoid of rapid oscillations) strongly suggest that this is the case.

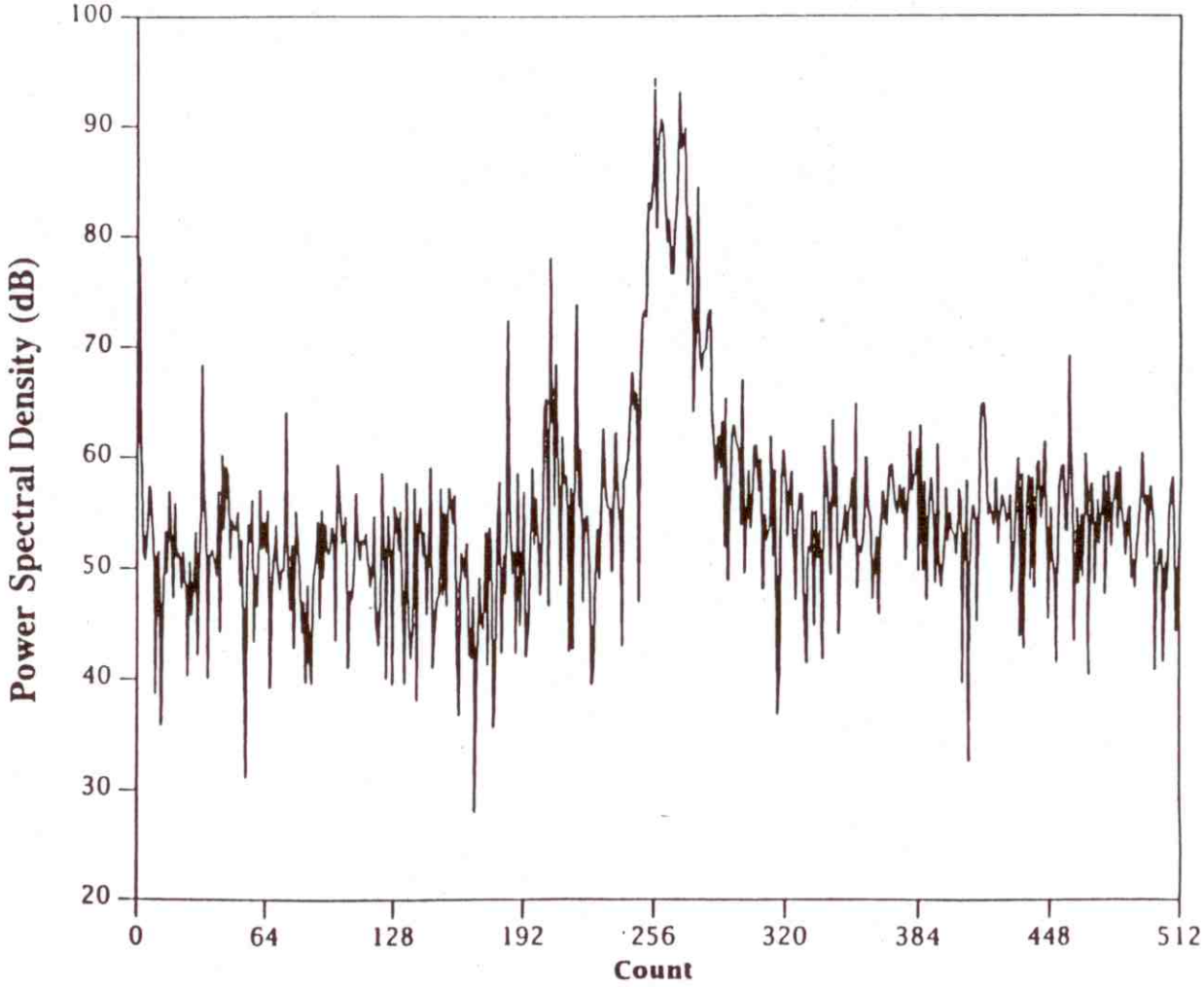

Figure 10. Power spectrum of measured noise/interference on a scale from 0 to 125 kHz (case study 3).

The I-channel data, the normalized autocorrelation function, and the average power for the fourth case study are shown in Figures 11, 12, and 13, respectively. As discussed in Part I, the noise/interference in this case is dominated by a single narrowband interferer. Thus, one expects the sum over narrowband interferers in (13) and (14) to be dominated by a single term, so that the magnitude of the autocorrelation function is approximately constant. As can be seen in Figure 12, the magnitude of the autocorrelation function is approximately constant over the first 8 ms, with small periodic oscillations. By the end of the record, the magnitude of the autocorrelation function has increased and is varying, although the structure and magnitude of the oscillations appears unchanged, indicating that the power of the dominant interferer has increased and is varying, whereas the power of the interferers responsible for the oscillations in the autocorrelation function have remained relatively stationary. Figure 13 reveals that the total power in the channel did indeed become oscillatory approximately half way through the record.

Figures 14, 15, and 16 show the I-channel data, the normalized autocorrelation function, and the average power, respectively, for the fifth case study. In this case the noise/interference includes impulsive noise in addition to narrowband interferers, as can be seen in Figure 14. However, the nature of the autocorrelation function (an impulse at $\tau=0$ followed by a periodic oscillatory function) is similar to the other case studies. This is because, as explained above, the impulses are narrow and do not arrive precisely periodically in time. The autocorrelation function in Figure 15 appears to change only slightly by the end of the record, indicating a relatively stationary channel. This is consistent with Figure 16, which shows that the fluctuations of the average power remain relatively stationary over the duration of the record, except for a noise burst approximately three fourths of the way through the record.

Based upon the case studies, it appears that the measured data have autocorrelation functions whose characteristics are well-described by (14) (with the exception of nonstationarity). Although (14) is also expected to correspond to the autocorrelation functions of the proposed noise/interference model, it remains to show that the simulated autocorrelation functions closely resemble those of the measured data. To verify this, a variety of simulations were conducted, both with and without impulsive noise.

Figure 17 shows plots of the magnitude of the normalized autocorrelation functions for simulated noise/interference consisting of Gaussian noise and narrowband interferers. As was

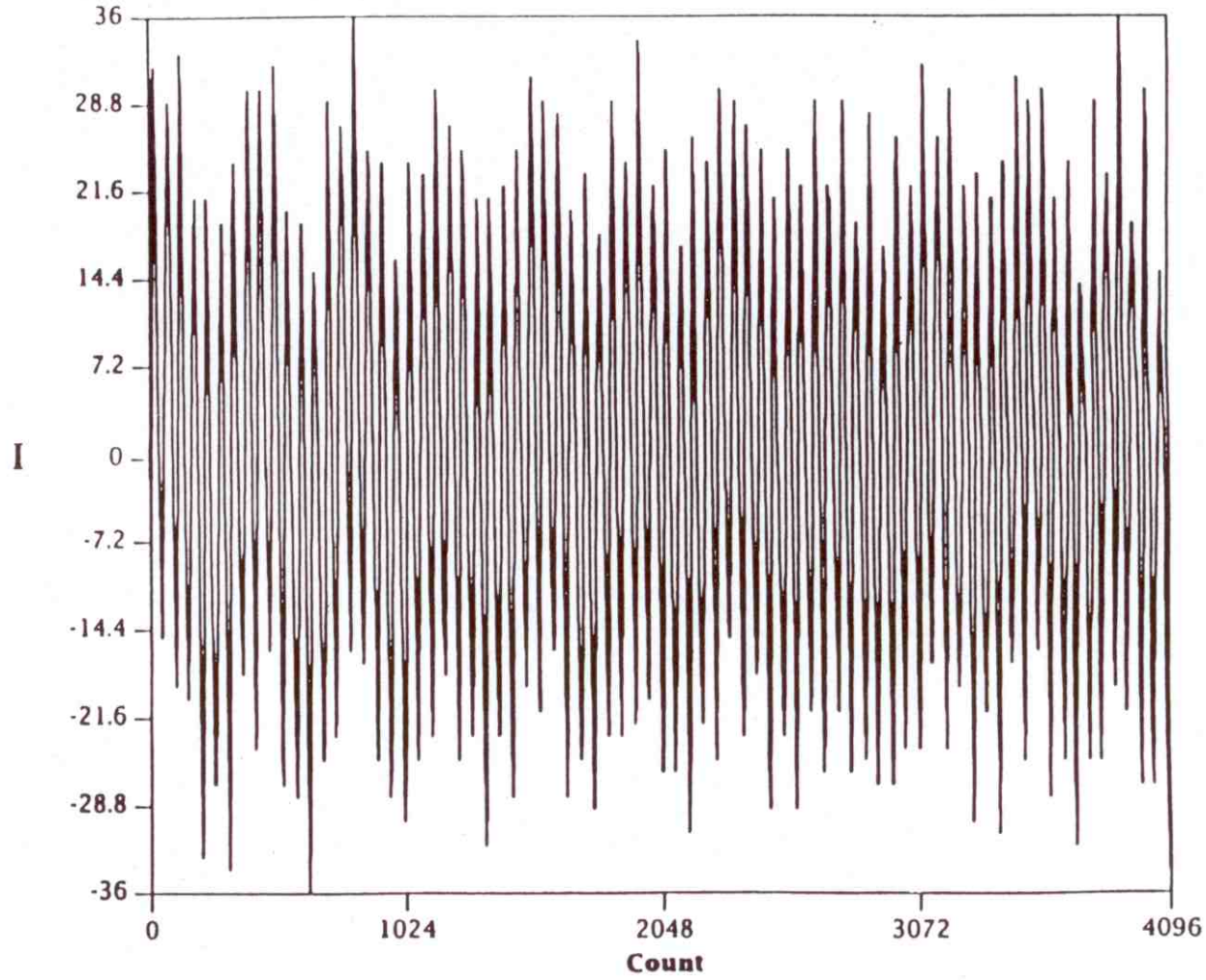

Figure 11. I-channel data at 13.666 MHz (case study 4).

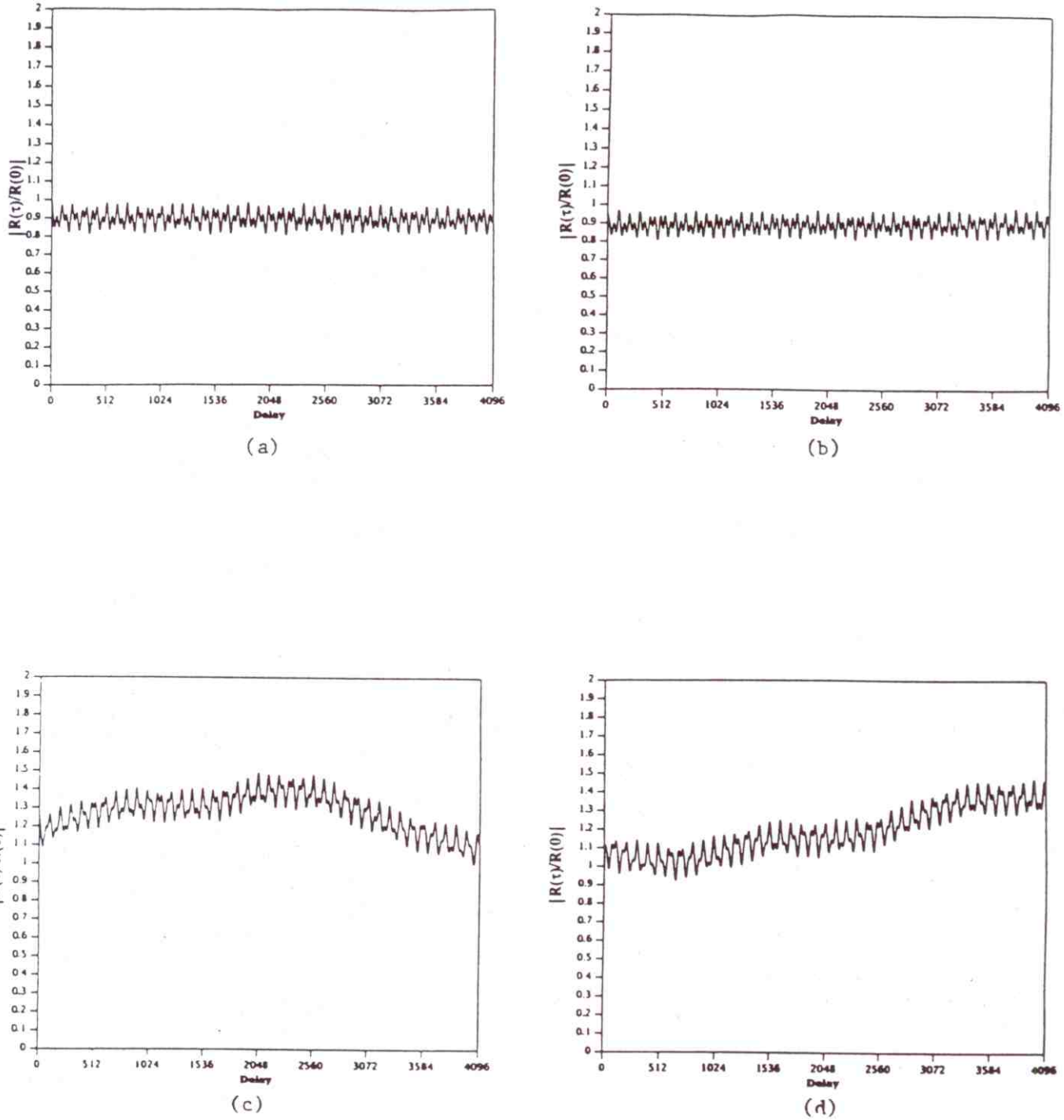

Figure 12. Normalized autocorrelation function for (a) $0 \leq \tau \leq 4$ms, (b) 4ms $\leq \tau \leq 8$ms, (c) 0.996s $\leq \tau \leq 1.0$s, and (d) 1.0s $\leq \tau \leq 1.004$s (case study 4).

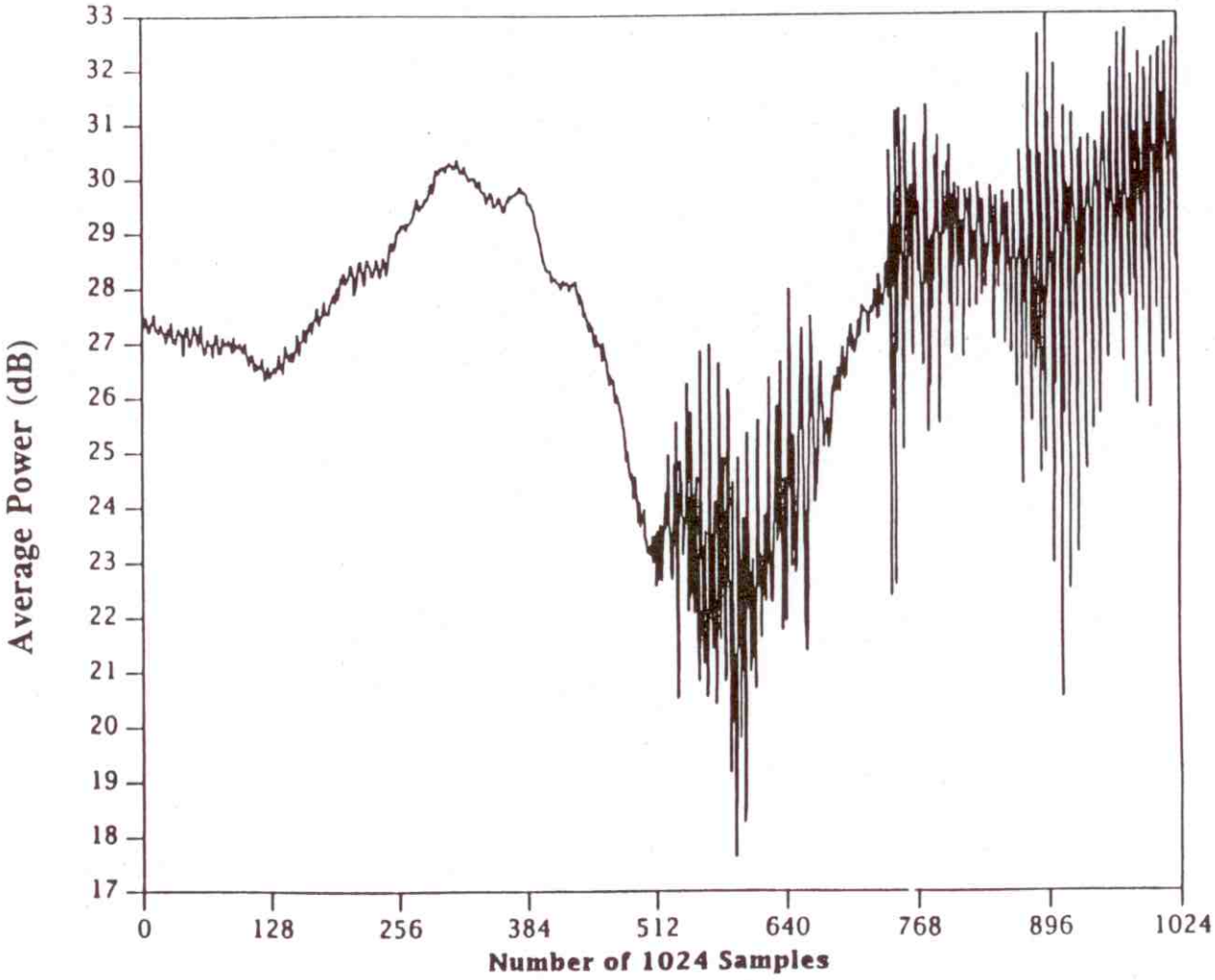

Figure 13. Average power of measured noise/interference (case study 4).

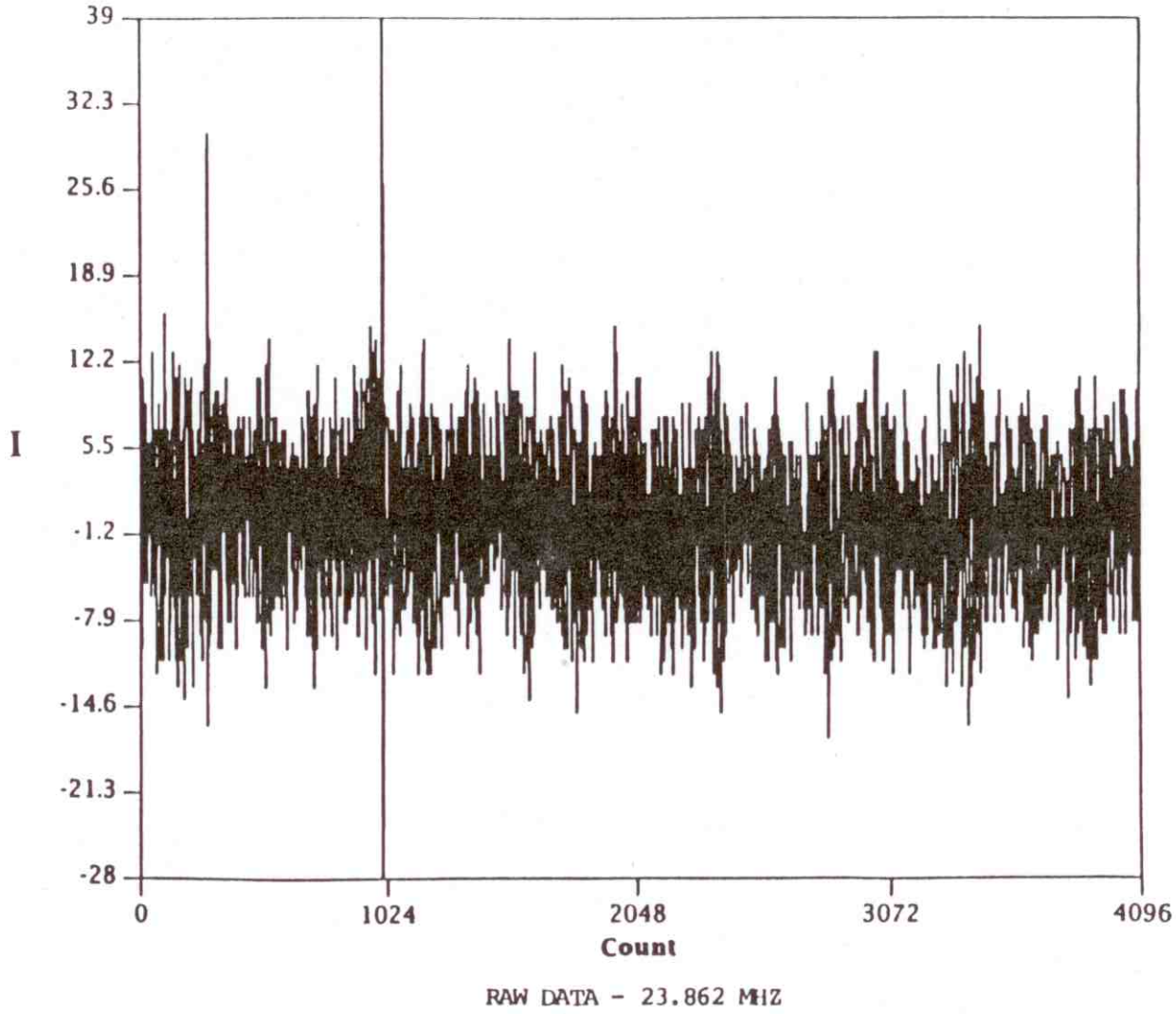

Figure 14. I-channel data at 23.862 MHz (case study 5).

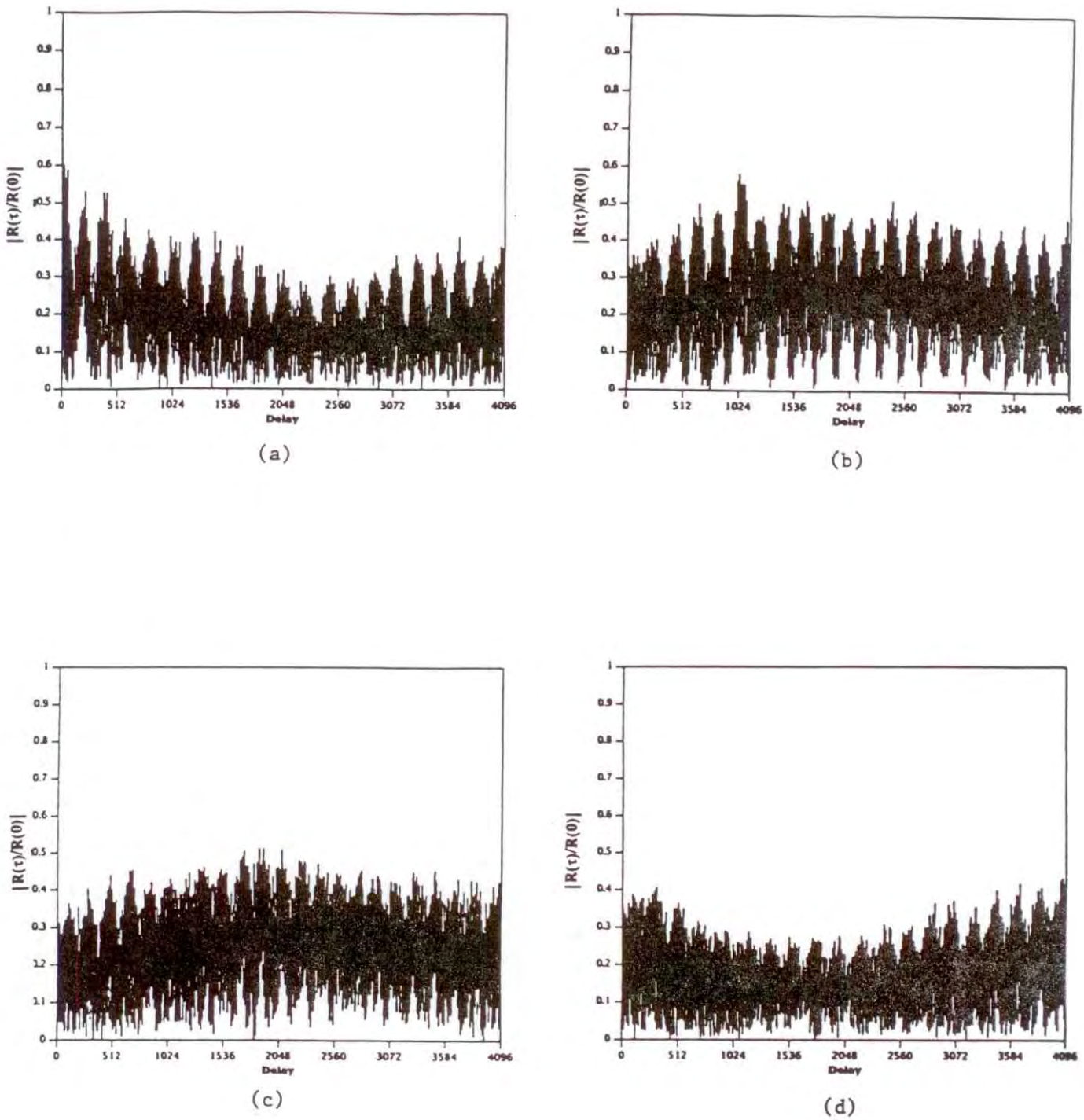

Figure 15. Normalized autocorrelation function for (a) $0 \leq \tau \leq 4$ms, (b) 4ms $\leq \tau \leq$ 8ms, (c) 0.996s $\leq \tau \leq$ 1.0s, and (d) 1.0s $\leq \tau \leq$ 1.004s (case study 5).

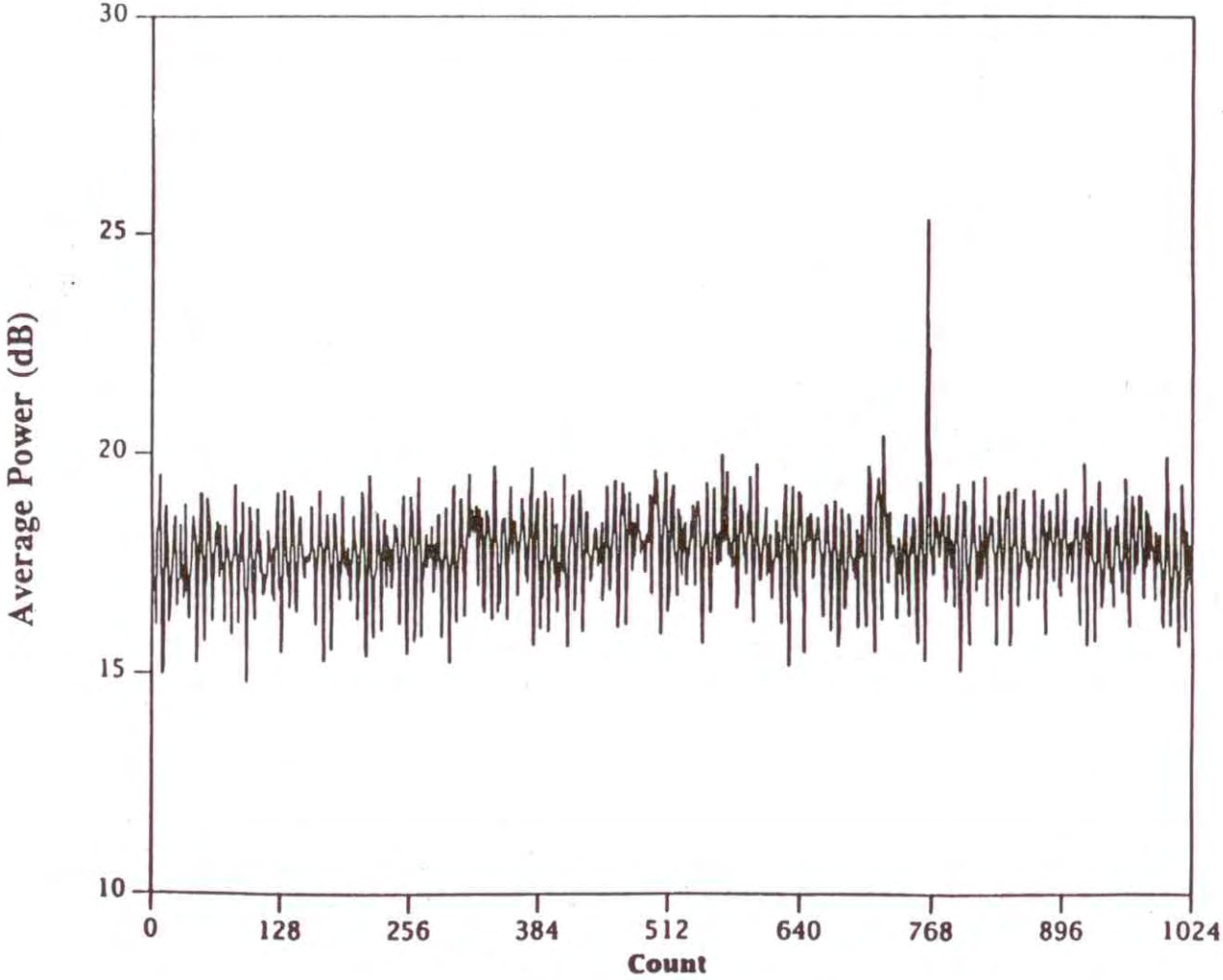

Figure 16. Average power of measured noise/interference (case study 5).

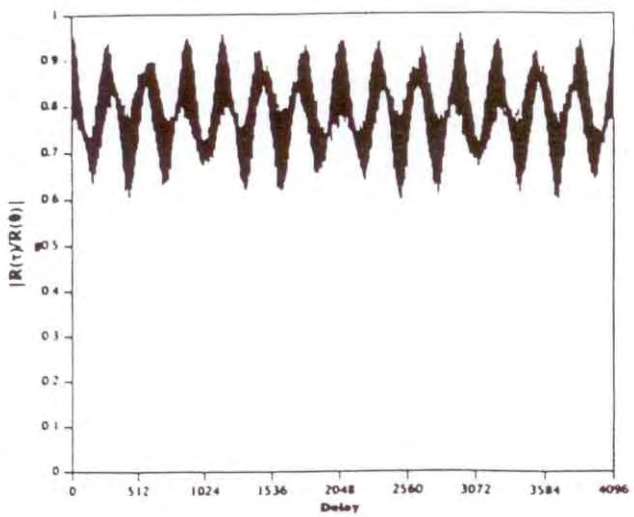

(a)

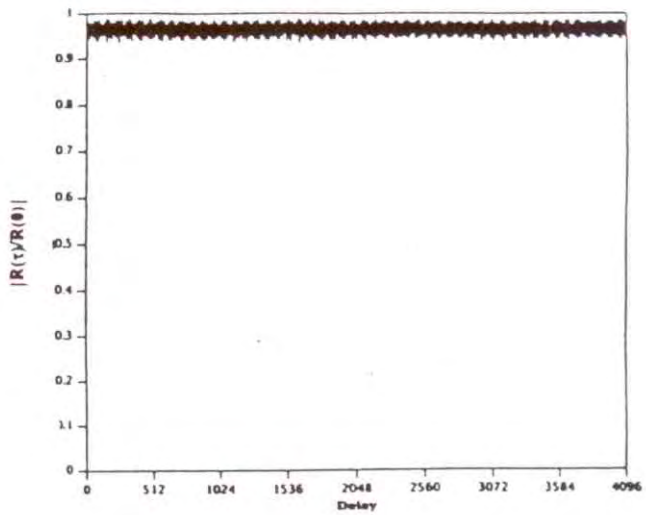

(b)

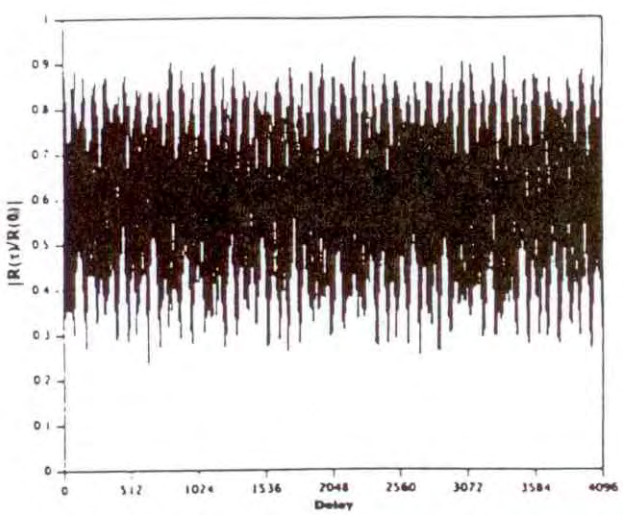

(c)

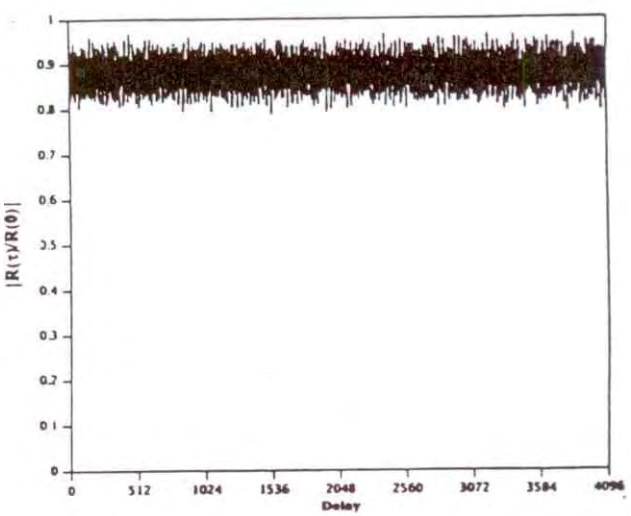

(d)

Figure 17. Normalized autocorrelation functions of simulated noise/interference (Gaussian noise and narrowband interferers).

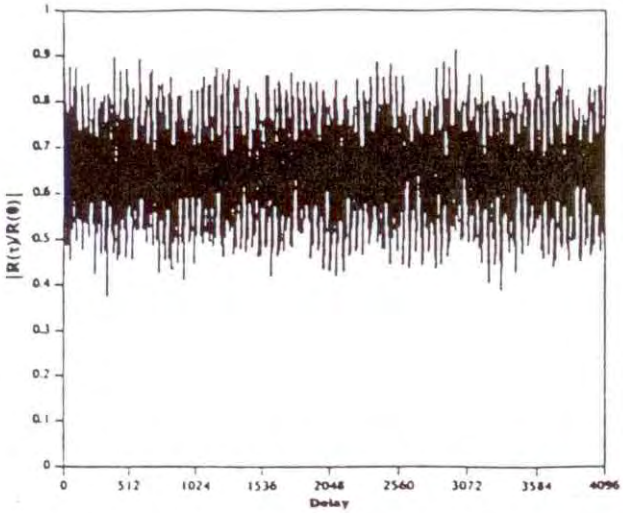

(e)

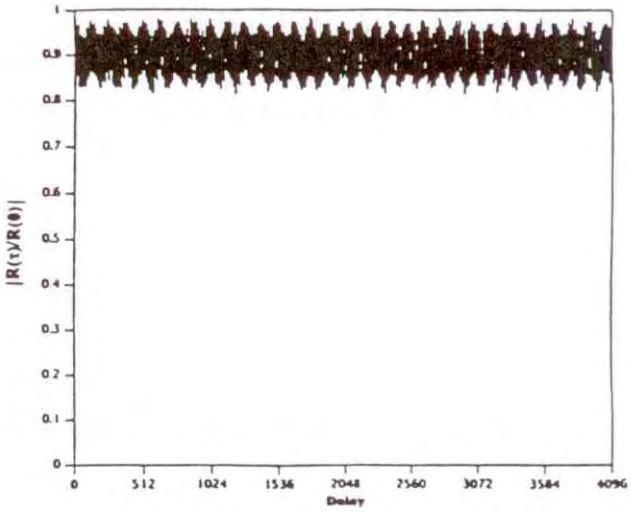

(f)

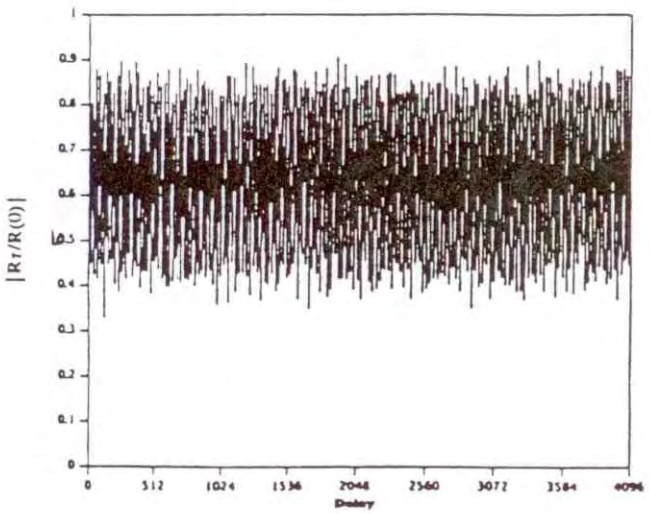

(g)

Figure 17. Normalized autocorrelation functions of simulated noise/interference. (cont.)

done for the case studies, the autocorrelation functions were computed using (8) with T=4 ms. Each plot shows an autocorrelation function for $0 \leq \tau \leq 4$ ms. The values of the model parameters are listed in Table 2, and are the same as those used in Part I to simulate noise/interference whose first-order statistics resemble those of the first case study. The examples in Figure 17 differ from one another only in the values of the random seeds used to generate the Gaussian noise and the frequencies, phases, and amplitudes of the narrowband interferers.

As expected, the normalized autocorrelation functions consist of a unit impulse at τ=0, followed by an approximately periodic function of τ. Like the autocorrelation functions of the measured data, the simulated autocorrelation functions exhibit a variety of different structures, although none of the simulated autocorrelation functions closely resembles any of the measured functions in quantitative detail. Such comparisons are admittedly qualitative, and do not constitute proof that the model can generate noise/interference waveforms which are identical (or nearly identical) to any and all of the waveforms observed in nature. The difficulty in achieving such a goal arises from the fact that one is dealing with random processes from numerous sources and environments, and therefore an infinite variety of waveforms. Thus, the purpose of the comparisons throughout this work (and in Part I as well) is not to simulate results which are identical to the measured results, but to demonstrate that, for representative examples, the model is capable of generating noise/interference whose statistical properties are similar to those of the measured data.

Table 2. Parameters Used in the Simulation Model for Figures 17 and 39 - 41

Parameter	Value
σ	0.12
N_i	39
γ_A	0.30
Θ_A	2.00

Figure 18 shows examples of autocorrelation functions for noise/interference consisting of Gaussian noise, narrowband interferers, and impulsive noise. The values of the model parameters are listed in Table 3, and are the same as those used in Part I to simulate noise/interference whose first-order statistics resemble those of the fifth case study. Again, the different examples in Figure 18 differ only in the values of the random seeds used to generate the noise/interference. As expected, the presence of impulsive noise randomly distributed in time does not appear to have any effect on the autocorrelation functions.

It remains to show that the model can generate noise/interference whose autocorrelation function resembles that of the third case study (Figure 8). To do so, noise/interference was simulated as follows. First, Gaussian noise (σ=1) was combined with 44 narrowband interferers (γ_A=0.2, θ_A=2.0). Then, the result was combined with a cluster of 5 dominant interferers whose amplitudes, phases, and frequencies are symmetrically distributed about the center of the cluster. Finally, the strongest of the original 44 interferers were excised to ensure that the cluster of 5

Table 3. Parameters Used in the Simulation Model for Figures 18 and 42 - 46

Parameter	Value
σ	0.12
N_i	39
γ_A	0.20
Θ_A	2.00
N_j	49/4 ms
γ_B	1.0×10^{-8}
Θ_B	1.20
B	400 kHz
B_{max}	2.0×10^{-5}

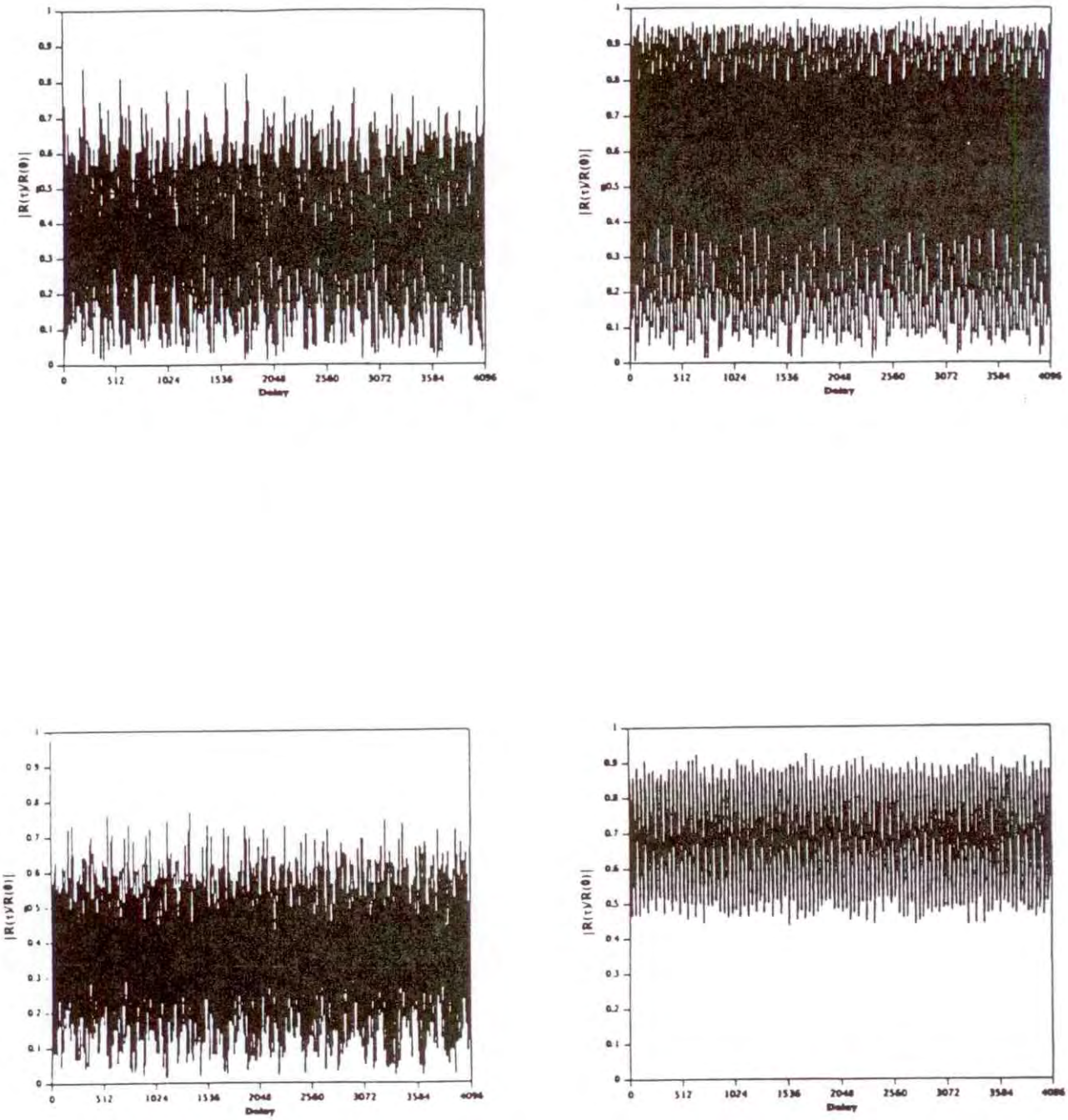

Figure 18. Normalized autocorrelation functions of simulated noise/interference (Gaussian noise, anrrowband interferers, and impulsive noise).

interferers dominates the power in the channel. The resulting power spectrum is shown in Figure 19. That portion of the power spectum containing the cluster of interferers is plotted on an expanded scale (-128 kHz to 0) in Figure 20, which resembles, but is not identical to, the spectrum in Figure 10. The first 4 ms of the simulated I-channel data are plotted in Figure 21, and resemble a single carrier with amplitude modulation, as do the data in Figure 7. The magnitude of the normalized autocorrelation function is shown in Figure 22 for $0 \leq \tau \leq 4$ ms. There are no rapid oscillations, as in the autocorrelation functions of the other simulated examples, and neither the I-channel data nor the autocorrelation function are periodic over the first 4 ms. Thus, an appropriate combination of narrowband interferers can result in an autocorrelation function similar to that in the third case study.

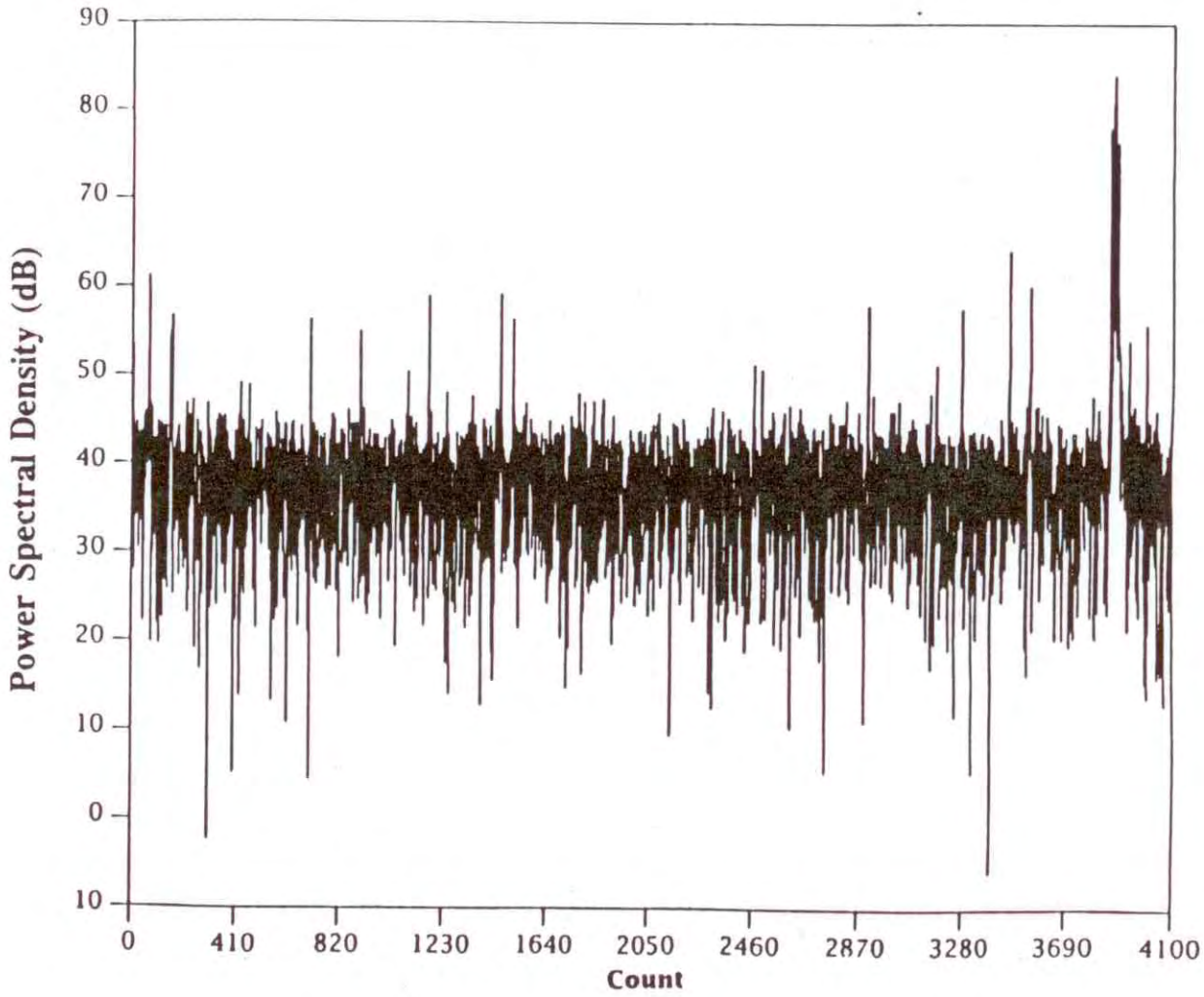

Figure 19. Power spectrum of simulated noise/interference over a bandwidth of 1.024 MHz.

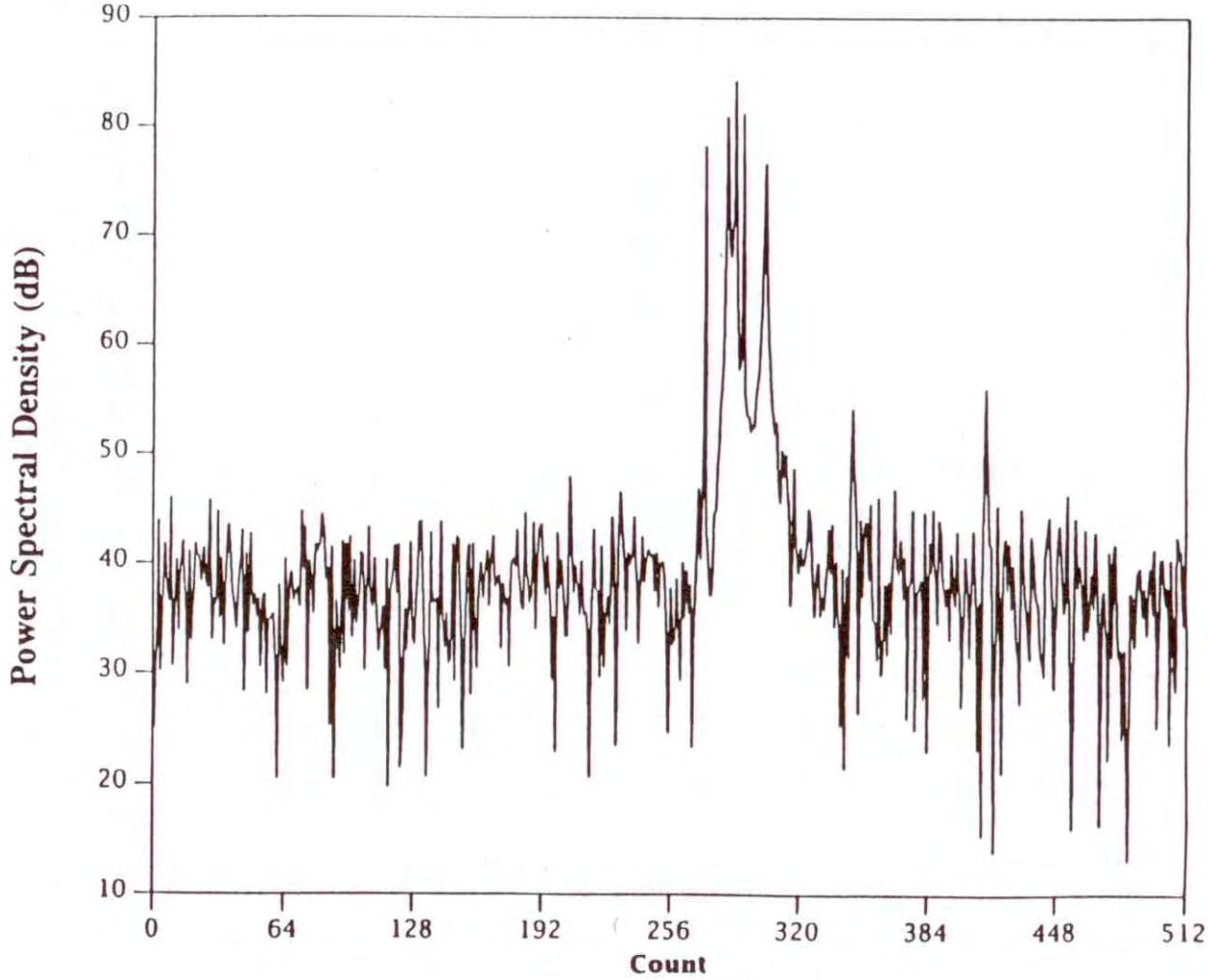

Figure 20. Power spectrum of simulated noise/interference on a scale from -125kHz to 0

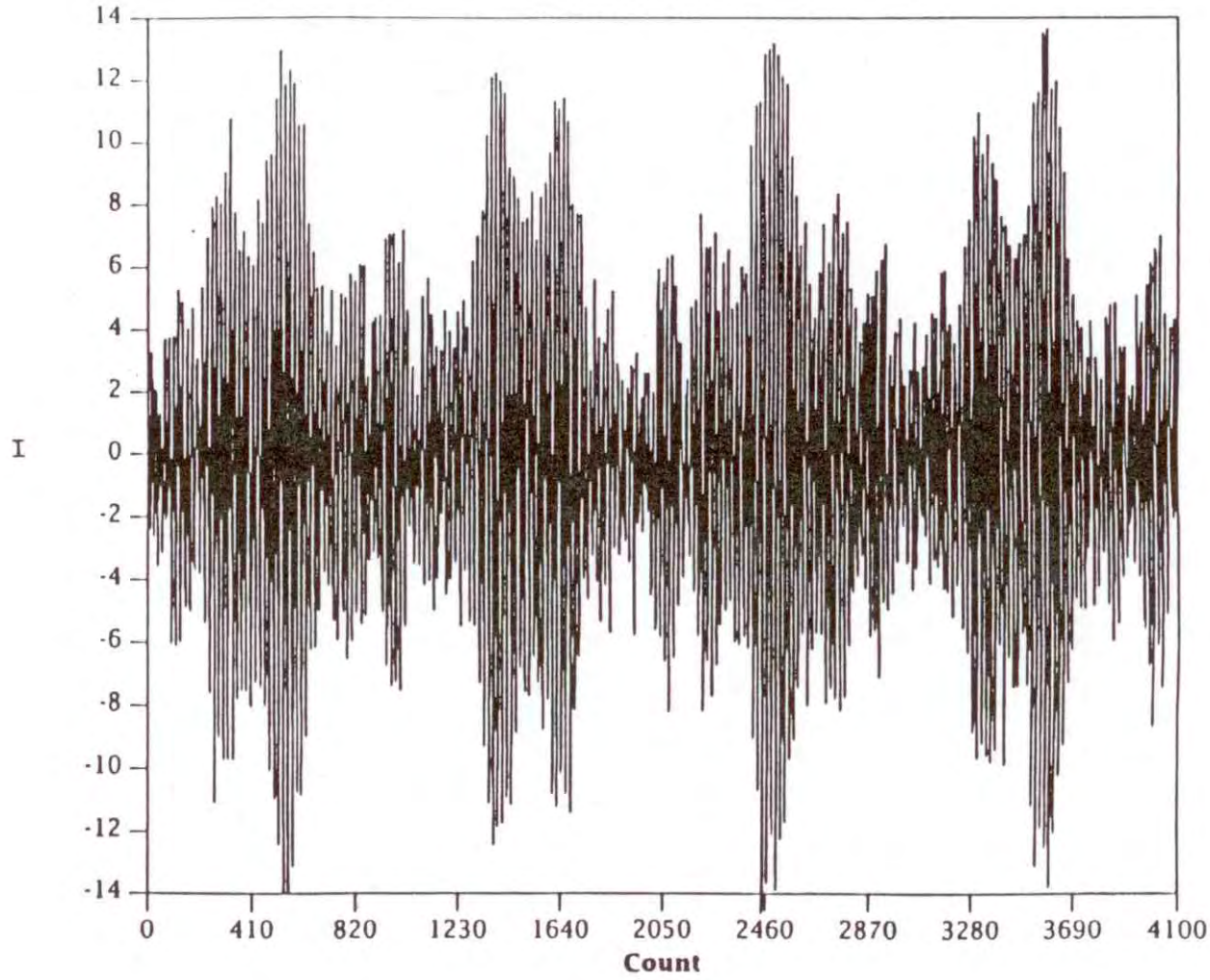

Figure 21. I-channel data of simulated noise/interference.

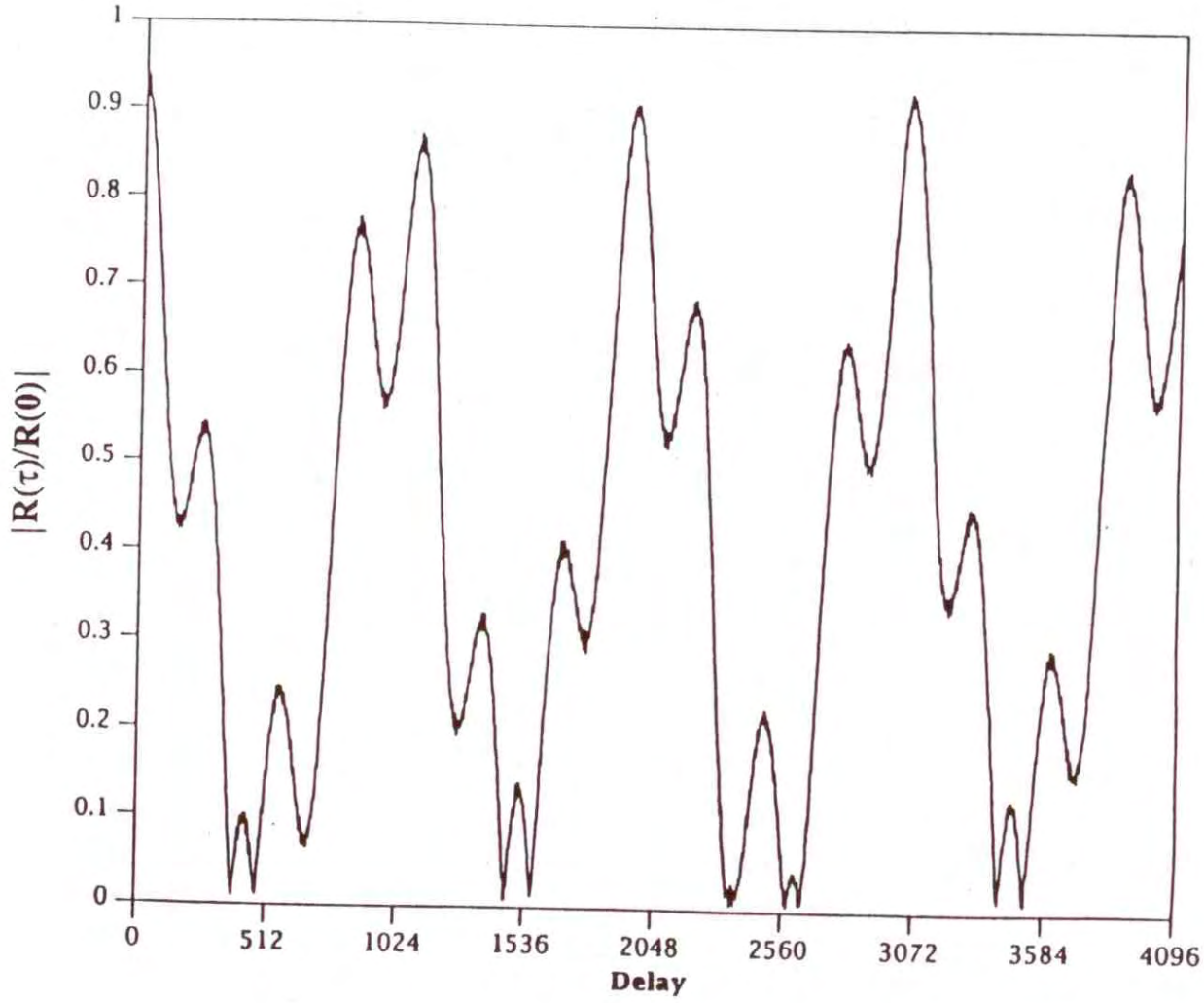

Figure 22. Normalized autocorrelation function of simulated noise/interference.